Gregory A. Campbell
Mark A. Spalding

Analyzing and Troubleshooting Single-Screw Extruders

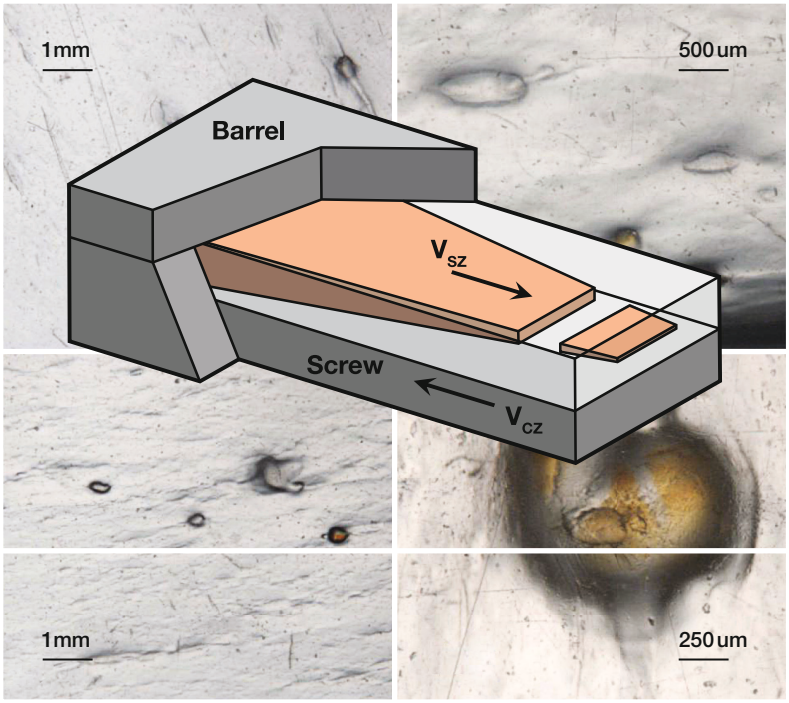

2nd Edition

HANSER

Campbell / Spalding
Analyzing and Troubleshooting Single-Screw Extruders

Gregory A. Campbell
Mark A. Spalding

Analyzing and Troubleshooting Single-Screw Extruders

2nd Edition

HANSER

Hanser Publishers, Munich

Hanser Publications, Cincinnati

The Authors:

Gregory A. Campbell, Ph. D.
Chief Technical Officer, Castle Associates, 1145 Mason Bay Road, Jonesport, ME 04649, USA

Mark A. Spalding, Ph. D.
Fellow, Dow, Inc., 1702 Building, Midland, MI 48667, USA

Distributed in the Americas by:
Hanser Publications
414 Walnut Street, Cincinnati, OH 45202 USA
Phone: (800) 950-8977
www.hanserpublications.com

Distributed in all other countries by:
Carl Hanser Verlag
Postfach 86 04 20, 81631 Munich, Germany
Fax: +49 (89) 98 48 09
www.hanser-fachbuch.de

Library of Congress Control Number: 2020946059

Editor: Dr. Mark Smith
Production Management: Der Buchmacher, Arthur Lenner, Windach
Coverconcept: Marc Müller-Bremer, www.rebranding.de, Munich
Coverdesign: Max Kostopoulos
Typesetting: Kösel Media GmbH, Krugzell, Germany
Printed and bound by CPI books GmbH, Leck
Printed in Germany

ISBN: 978-1-56990-784-9
E-Book ISBN: 978-1-56990-785-6

Preface

Classically, all prior extrusion books are based on barrel rotation physics. Literature developed over the past 15 years has led to this first book to be published based on the actual physics of the process—screw rotation physics. After the theories and the math models are developed in the first nine chapters, the models are then used to solve actual commercial problems in the remainder of the book. Realistic case studies are unique in that they describe the problem as viewed by the plant engineers and provide the actual dimensions of the screws. Knowledge is developed using a series of hypotheses that are developed and then tested, which allows a series of technical solutions. Several actual solutions are proposed with the final results that solve the problem then clearly presented. Overall, there is not a book on the market with this level of detail and disclosure. New knowledge in this book will be highly useful for production engineers, technical service engineers working with customers, consultants specializing in troubleshooting and process design, and process researchers and designers that are responsible for processes that run at maximum rates and maximum profitability.

Debugging and troubleshooting single-screw extruders is an important skill set for plant engineers since all machines will eventually have a deterioration in their performance or a catastrophic failure. Original design performance must be restored as quickly as possible to mitigate production losses. With troubleshooting knowledge and a fundamental understanding of the process, the performance of the extruder can be restored in a relatively short time, minimizing the economic loss to the plant. Common root causes and their detection are provided. Hypothesis testing is outlined in Chapter 10 and is used throughout the troubleshooting chapters to identify the root causes. Elimination of the root cause is provided by offering the equipment owner several technical solutions, allowing the owner to choose the level of risk associated with the process modification. Mechanical failures are also common with single-screw extruders, and the common problems are identified. Illustrations are provided with the problems along with many numerical simulations of the case studies. Collectively, these instruct the reader on how to determine and solve many common extrusion problems. About 100 case studies and defects are identified in the book with acceptable technical solutions. Lastly, we

hope that this book provides the information and technology that is required for the understanding, operation, and troubleshooting of single-screw extruders.

We have focused on two things as we developed the second edition of this treatise on single-screw fundamentals and application of those fundamentals to the engineering art of troubleshooting, research/development, and production single screw extruders. The stoichiometry of several important chemical reactions relating to the number of important commercial polymer monomers and their polymers was addressed in Chapter 2. Also, in Chapter 2 a table of 10 commercial polymers and their properties and structure was added so the reader can relate to some important polymers finished properties after extrusion. With the constraint of few new monomers and the cost and risk of building new monomer and polymer plants, the polymer industry has been focusing on developing rigid and fiber-based composite materials. A major addition to Chapter 3 is the development of an energy-based model for the shear thinning power law. The technique of using this new concept on polymer particulate composites is then developed and the utility of this concept is applied to the limiting extrusion-injection rate for injection molding. The difficulties of extruding a sound-deadening composite due to a filler change is related to the importance of understanding that filled system rheology is dependent on the volume and not the weight fraction of the filler. Other additions include an expansion of the design of Maddock mixers, transfer line designs, economic evaluations, and new case studies.

Gregory A. Campbell

Mark A. Spalding

Acknowledgements

My interest in fundamental polymer research began in 1964 when I began my graduate career. My research efforts were strongly influenced by my mentor Professor Edward G. Bobalek, one of finest gentleman and innovative research minds I have ever met. My research philosophy was strongly influenced by many encounters with Ed before and after I defended my dissertation. One particularly important encounter occurred when I was lamenting that my dissertation research did not appear to be a really important breakthrough. He took a long draw on his ever present pipe and said "Greg, that is why we call it research and not search." From that time on I have always looked at my efforts as learning from the previous researchers that have laid the technical foundation in the area that is now being addressed. My role is thus to continue to build on that foundation when looking for a solution to the research challenge that I am currently addressing.

After leaving the University of Maine, I worked with wonderful groups of exceptional researchers at General Motors research, Mobil Chemical research, and Clarkson University. Many of these individuals spent their valuable time to help me hone my research skills. Probably the most influential individual was Dr. William Meluch; a true genius that I had the pleasure of working with for 13 years. Another good friend that had a major influence on my manner of approaching engineering research was Professor Art Fricke whom I collaborated with at the University of Maine and the University of Florida. My colleague Dr. Don Rassmussen at Clarkson University provided important guidance in all things thermodynamic.

My extrusion experience started when I directed process research at Mobil Chemical Research in the early 1980s. We developed and analyzed data on a 24 to 1 single-screw extruder with 12 infrared probes and 12 pressure probes using high-speed data acquisition. I then changed career paths and accepted a position at Clarkson University teaching chemical engineering while developing the Clarkson Polymer Processing Laboratory. The new concepts developed in this book were first recognized by Dr. Paul Sweeney when he was a graduate student in about 1988. I have to admit that it took considerable effort on Paul's part to convince me to even address these new concepts. Once we became convinced that it was important to complete the solution of the single-screw extruder analysis and bring the solution

back to the laboratory frame, it has taken 25 years to reach our current incomplete understanding. I would not have been able to acquire this understanding without the dedication and efforts of my colleagues and students that led the extrusion research in my lab: Paul Sweeney, Jeff Felton, Douglas Small, ChiCheng Wang, Dontula Narasimharao, Diana Hunt, Hongying Cheng, Zirong Tang, Mary Ann te-Riele, Jason C. Baird, Sirisha Bomma, and Sam St. John. An academic without excellent students is severely handicapped and I can truly say that I was not handicapped.

The development of this book has been an interesting and exhausting "trip" which in all likelihood would not have been completed without the encouragement and understanding of Sue, my wife for the past 50 years.

Gregory A. Campbell, Castle Research, Jonesport, Maine

My extrusion career started as one of the founding members of the Polymer Processing Technology Team of The Dow Chemical Company in 1987. The team was built and led by Dr. Kun Sup Hyun and consisted of four members (along with Joseph Dooley and Thomas McCullough). During the early years, the team researched many aspects of polymer processing including single-screw extrusion, twin-screw extrusion, and die technologies. These early years allowed the team to develop strong skills in process fundamentals, design, and troubleshooting. I am grateful to have this experience and the opportunity to develop this skill set. I am also grateful for the many mentors that I have had through my life including my father, Robert Bean, Gene Kratzman, Prof. Lyle F. Albright, and Dr. Hyun.

A book like this would not be possible without the help and contributions from coworkers, industry experts, and family. Many of the figures were contributed by industry experts and their names are provided with the figure. Photographs, content, and assistance were provided by Timothy W. Womer (consultant), Jeffery Kuhlman (Glycon), Jeff Myers (Robert Barr, Inc.), James Fogharty (Plastics Engineering Associates Licensing, Inc.), John Christiano (Davis-Standard), William Kramer (American Kuhne), and many others. Numerous diagrams were made and enhanced by my sons Stephen W. Spalding and Aaron F. Spalding. I also thank those who reviewed the original chapter drafts.

My wife Pamela has been a source of inspiration and motivation during this project. I thank her and my sons for their continued support through the writing of this book. My parents William and Joan provided me with a loving environment while growing up, and they provided the foundation for success.

Mark A. Spalding, The Dow Chemical Company, Midland, MI

Contents

1 Single-Screw Extrusion: Introduction and Troubleshooting

This book was written to provide the extrusion process engineer with a resource for assessing and fixing process problems associated with the use of single-screw extruders. The authors have drawn on their complementary backgrounds; both have worked with industrial extruder design, analysis, and fundamental research in the mechanism, operation, and troubleshooting of the single-screw extrusion process. The use of single-screw extruders in production processes has progressed significantly over the past several decades. As a result, the number of single-screw extruders in use has increased dramatically as has the diameter and length of the machine, especially for melt-fed extruders used in large resin production plants. In addition, resin manufacturers have developed many new resins for final products such as extruded sheet, film, pipe, fibers, coatings, and profiles. The extruder is still the process unit of choice for producing pellets in the production of polymer materials. Two types of extruders are generally used in polymer production: single-screw extruders and twin-screw extruders. The material in this book will be confined to the analysis and troubleshooting of single-screw extruders. The rapid expansion of this part of the polymer industry has been accompanied by the need for many new extrusion engineers. Many of these engineers have not had formal training in the analysis of the extruder and screw design nor have they had extensive education in polymer materials, which would help in troubleshooting problems on production equipment.

All single-screw extruders have several common characteristics, as shown in Figure 1.1 and Figure 1.2. The main sections of the extruder include the barrel, a screw that fits inside the barrel, a motor-drive system for rotating the screw, and a control system for the barrel heaters and motor speed. Many innovations on the construction of these components have been developed by machine suppliers over the years. A hopper is attached to the barrel at the entrance end of the screw and the resin is either gravity-fed (flood-fed) into the feed section of the screw or metered (starve-fed) through the hopper to the screw flights. The resin can be in either a solid particle form or molten. If the resin feedstock is in the solid form, typically pellets (or powders), the extruder screw must first convey the pellets away from the feed opening, melt the resin, and then pump and pressurize it for a

downstream process operation. This type of machine is referred to as a plasticating single-screw extruder. The barrel is usually heated with a minimum of three temperature zones. These different temperature zones are consistent with the three utilitarian functions of the screw: solids conveying, melting, and pumping or metering of the polymer.

Figure 1.1 Photograph of a highly instrumented 63.5 mm diameter extruder built by American Kuhne

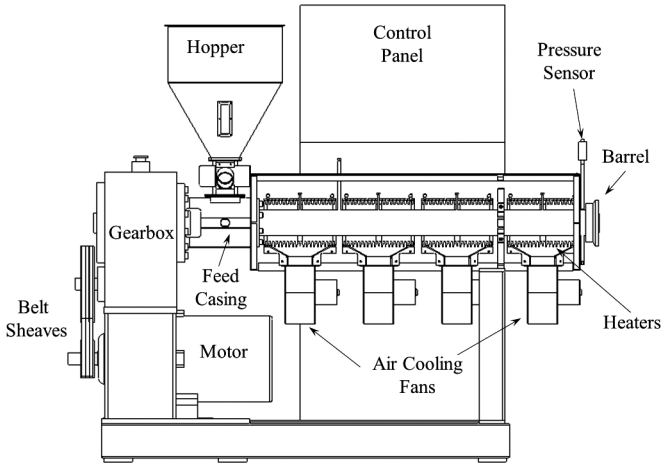

Figure 1.2 Schematic of a typical plasticating single-screw extruder. The extruder is equipped with four barrel heating and cooling zones and a combination belt sheave gearbox speed reduction drivetrain (courtesy of William Kramer of American Kuhne)

The single-screw plasticating process starts with the mixing of the feedstock materials. Typically, several different feedstocks are added to the hopper, such as fresh resin pellets, recycle material, additives, and a color concentrate. The recycle material typically comes from the grinding of edge trim, web material from thermo-

forming processes, or off-specification film and sheet. Often these components need to be dried and blended prior to adding them to the hopper. Next, the feedstock flows via gravity from the hopper through the feed throat of the feed casing and into the solids-conveying section of the screw. Typically this feed casing is cooled using water. The feed section of the screw is typically designed with a constant depth and is about 4 to 8 barrel diameters in axial length. Directly after the solids-conveying section is a section where the channel depth tapers to a shallow depth-metering section. The tapered-depth section is commonly referred to as the transition or melting section. In general, the metering section is also a constant depth, but many variations exist where the channels oscillate in depth. The metering section pumps and pressurizes the material for the downstream unit operations, including static mixers, screen filtering devices, gear pumps, secondary extruders, and dies. The total length of the extruder screw and barrel is typically measured in barrel diameters or as a length-to-diameter (L/D) ratio. Section lengths are often specified in barrel diameters or simply diameters.

The plasticator on an injection-molding machine is a specialized plasticating single-screw extruder. The plasticator has two main differences: there is a nonreturn valve on the tip of the screw, and the screw retracts as molten material accumulates between the nonreturn valve and the end of the barrel. Pressure is maintained on the accumulated material by a constant force applied to the shank of the screw via the drive system. This force is typically measured as a pressure applied to the shank and is referred to as the "back pressure." During the injection step of the process, the screw is forced forward, the nonreturn valve closes, and the material is injected into the mold. Additional information on the injection-molding process can be obtained elsewhere [1].

1.1 Organization of this Book

This book has been organized so that the information is helpful in troubleshooting extruders and extrusion processes, and it is presented in a manner that is of maximum utility to extrusion engineers. Appendices have been provided that present the theoretical analysis and assumptions in developing the design equations used throughout this text. In order to assess extruder production problems, it is necessary to understand the nature of the polymer that is being extruded, the design of the extruder and screw, and the interaction of these as the extruder is being operated. Numerous case studies are presented that demonstrate these interactions.

Knowledge of the geometry and mathematical description of a screw is required to understand the analysis of the functional sections of the screw and the trouble-

shooting of case studies. In Chapter 1 the geometry and mathematical descriptions are presented. Also in this chapter, the calculation of the rotational flow (also known as drag flow) and pressure flow rates for a metering channel is introduced. Simple calculation problems are presented and solved so that the reader can understand the value of the calculations.

Resin manufacturers go to extreme measures to produce a reproducible, high-quality, and useful polymer that is ready for final conversion to a product. Every time these polymers are passed through an extruder, however, the polymer has the potential to degrade, changing the chemical and physical properties of the resin. Degradation processes can often be the cause of extrusion problems. Chapter 2 begins with an introduction to how polymers are produced from the perspective of the type of chemical bonds that are important in different polymer families. It is beyond the scope of this book to discuss polymer production processes in detail. The discussion of polymerization is intended to aid the reader with a basic understanding on how the polymer is formed from its monomer. Knowing how the polymer was produced from its monomers will provide the engineer with the knowledge of how the extrusion process interacts with the polymer. This basic understanding will help in troubleshooting situations where the problem is the effect of the extrusion process on the stability of the polymer being extruded.

The physical properties that are important to polymer processing are presented in Chapters 3 and 4. Chapter 3 provides a basic understanding of the viscoelastic characteristics of polymers. In this chapter the fundamental concepts of polymer rheology are developed, and then there is a discussion of Newtonian and Power Law rheological responses of polymeric fluids, followed by a short introduction to the elastic nature of polymer melts. Chapter 4 presents the remaining physical properties, including friction coefficients (or stress at an interface), densities, melting fluxes, and thermal properties. These properties impact the performance of a resin during the extrusion process.

The fundamental processes and mechanisms that control single-screw extrusion are presented in Chapters 5 through 8. These processes include solids conveying, melting, polymer fluid flow, and mixing. The analyses presented in these chapters focus on easily utilized functions needed to assess the operation of the single-screw extruder. The derivation of these relationships will be presented in detail in the appendices for those who desire to explore the theory of extrusion in more detail.

The remaining Chapters 9 through 15 are devoted to different types of extrusion troubleshooting analyses. These chapters include presentations on scale-up techniques, general troubleshooting, screw fabrication, contamination in finished products, flow surging, and rate limitations. The chapters are presented with actual case studies of extrusion troubleshooting problems with the detailed analytical approach that was used to address these problems. As part of this troubleshooting

presentation, high-performance screws and their benefits are presented. Lastly, melt-fed extruders will be discussed. Melt-fed extruders are a special class of machines that are rarely discussed in the open literature.

Appendix A1 has a listing of the polymer abbreviations used in this book.

1.2 Troubleshooting Extrusion Processes

All extrusion and injection-molding plastication processes will eventually operate at a performance level less than the designed level. This reduction in performance can be caused by many factors, including but not limited to control failures, a worn screw or barrel, or a process change such as processing a different resin. Moreover, an improper screw design or process operation can limit the performance of the machine and reduce the profitability of the plant. Other processes may be operating properly at the designed rate, but a higher rate may be required to meet market demands. In this case, the rate-limiting step of the process needs to be identified and a strategy developed to remove the limitation.

Troubleshooting is a process for systematically and quickly determining the root cause of the process defect. The troubleshooting process is built on a series of hypotheses, and then experiments are developed to prove or disprove a hypothesis. The ability to build a series of plausible hypotheses is directly related to the knowledge of the engineer troubleshooting the process. Our focus is on providing the knowledge for the proper operation of an extrusion process, helping determine typical root causes that decrease the performance of the machine, and offering methods of removing the root cause defect from the process.

The economic impact of a properly designed troubleshooting process can be significant, especially if the defect is causing very high scrap rates or production requirements are not being met. Returning the process to full production in a timely manner will often require subject matter experts from several disciplines or companies. An excellent example of a troubleshooting process is described next for a processing problem at the Saturn Corporation.

1.2.1 The Injection Molding Problem at Saturn

During the startup of Saturn Corporation's Spring Hill, Tennessee, plant in September of 1990, a serious splay problem was encountered for the injection molding of door panels from a PC/ABS resin [2]. Splay is a common term used to describe surface defects on injection-molded parts. The splay on the surface of the door

panels created parts with unacceptable appearances after the painting process. The part rejection rate was higher than 25%, high enough to nearly shut down the entire plant. Teams were formed from the companies involved to determine quickly the root cause for the splay. After a detailed analysis was performed, it was determined that the plasticating screw in the injection molder was not operating properly, causing some of the resin to degrade in the channels of the screw. The splay was created by the volatile components from the degradation of the resin. A high-performance Energy Transfer (ET) screw [3] was designed and built, eliminating the splay. A detailed discussion of the troubleshooting process at Saturn is presented in Section 11.12.5.

The troubleshooting project at Saturn is an excellent example of combining strengths from different companies to diagnose and eliminate a costly defect from a process.

1.3 Introduction to Screw Geometry

In order to simulate an extrusion process or design a screw, the mathematical description of the screw geometry must be understood. This section provides the basic details that describe a screw and the complex mathematics that describe the channels.

The single-screw extruder screw can be single flighted or multiple flighted. A conventional single-flighted screw is shown in Figure 1.3. This screw has a single helix wound around the screw root or core. Multiple-flighted screws with two or more helixes started on the core are very common on high-performance screws and on large-diameter melt-fed machines. For example, barrier melting sections have a secondary barrier flight that is located a fraction of a turn downstream from the primary flight, creating two flow channels: a solids melting channel and a melt-conveying channel. Moreover, many high-performance screws have two or more flights in the metering section of the screw. Barrier screws and other high-performance screws will be presented in Chapter 14. Multiple flights are very common on larger-diameter extruder screws, because this creates a narrower channel for the polymer melt to flow through, leading to less pressure variation due to the rotation of the screw. In addition, the multiple flights spread the bearing forces between the flight tip and the barrel wall. Melt-fed extrusion processes will be discussed in detail in Chapter 15. The screw is rotated by the shank using either specially designed splines or by keys with rectangular cross sections. The mathematical zero position of the screw is set at the pocket where the screw helix starts. Most extruder manufacturers rotate the screw in a counterclockwise direction for

viewers positioned on the shank and looking towards the tip. This rotation convention, however, is not standard.

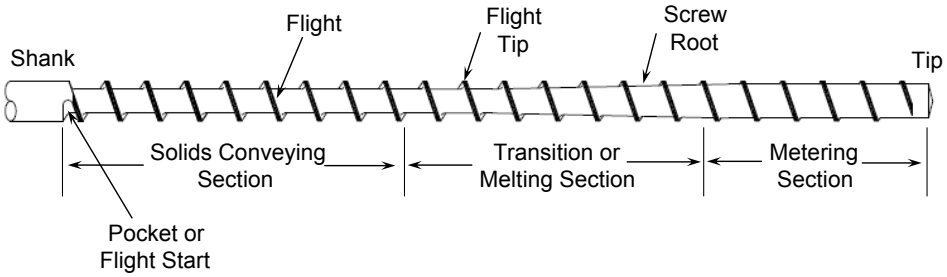

Figure 1.3 Schematic of a typical single-flighted screw (courtesy of Jeff A. Myers of Robert Barr, Inc.)

The flight is a helical structure that is machined into the screw and extends from the flight tip to the screw core or root. The flight has a width at the flight tip called the flight land. The small clearance between the flight land and the barrel wall minimizes the flow of polymer back toward the feed section. The polymer that does flow between the clearances supports the screw and centers it in the barrel. The radial distance between the flight tip and the screw root is referred to as the local flight height or channel depth. The feed section usually has a constant-diameter core that has the smallest diameter, the largest channel depth, and the largest cross-sectional volume in the screw. The deep channel conveys the relatively low bulk density feedstock pellets into the machine. The feedstock is conveyed forward into the transition section or melting section of the screw. The transition section increases in root diameter in the downstream direction, and thus the channel depth decreases. Here, the feedstock is subjected to higher pressures and temperatures, causing the feedstock to compact and melt. As the material compacts, its bulk density can increase by a factor of nearly two or more. As the feedstock compacts, the entrained air between the pellets is forced back and out through the hopper. For example, a pellet feedstock such as ABS resin can have a bulk density at ambient conditions of 0.65 g/cm^3 while the melt density at 250 °C is 0.93 g/cm^3. Thus for every unit volume of resin that enters the extruder, about 0.3 unit volumes of air must be expelled out through the voids in the solid bed and then out through the hopper. The transition section is where most of the polymer is converted from a solid to a fluid. The fluid is then conveyed to the metering section where the resin is pumped to the discharge opening of the extruder. In general, the metering section of a conventional screw has a constant root diameter, and it has a much smaller channel depth than the feed section. The ratio of the channel depth in the feed section to the channel depth in the metering section is often referred to as the compression ratio of the screw.

1.3.1 Screw Geometric Quantitative Characteristics

The book *Engineering Principles of Plasticating Extrusion* by Tadmor and Klein [4] has been used extensively in gaining an understanding of the fundamentals of extrusion processes. The following section endeavors to maintain the quality of the development of the screw geometry section of this classic text. Understanding the relationships between the screw geometry and the symbolic and mathematical representation of a screw is a critical beginning for understanding the rate, pressure, and temperature calculations. These functions related to the performance of single-screw extruders are developed later in this book and require an understanding of the screw geometry.

The geometry of a double-flighted screw and its nomenclature are presented in Figure 1.4 using the classical description from Tadmor and Klein [4]. The nomenclature has been maintained to provide consistency with the classical literature and to provide some generality in the development of the symbols and equations that are used in extruder analysis.

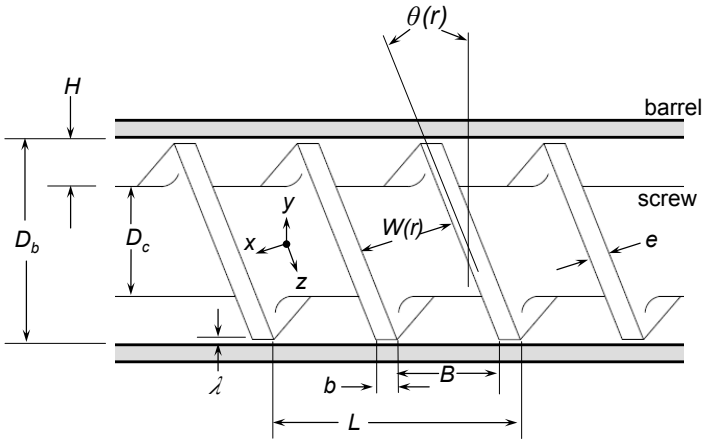

Figure 1.4 A schematic of a double-flighted screw geometry

Several of the screw geometric parameters are easily obtained by observation and measurement, including the number of flight starts, inside barrel diameter, channel depth, lead length, flight width, and flight clearance. The number of flight starts, p, for the geometry in Figure 1.4 is two. The inner diameter of the barrel is represented by D_b, and the local distance from the screw root to the barrel is H. The diameter of the screw core is represented by D_c. The mechanical clearance between the land of the screw flight and the barrel is λ. The mechanical clearance is typically very small compared to depth of the channel. The lead length, L, is the axial distance of one full turn of one of the screw flight starts. This is often constant in each section of the screw, but in some screws, such as rubber screws, it often con-

tinuously decreases along the length of the screw. A screw that has a lead length that is equal to the barrel diameter is referred to as square pitched. The flight width at the tip of the screw and perpendicular to the flight edge is e.

The remaining geometrical parameters are easily derived from the measured parameters presented above. Several of the screw parameters are functions of the screw radius. They include the perpendicular distance from flight to flight, $W(r)$; the width of the flights in the axial direction, $b(r)$; and the helix angle, $\theta(r)$, the angle produced by the flight and a plane normal to the screw axis. These parameters will be discussed later. At the barrel wall these parameters are subscripted with a b. The helix angle at the barrel wall is θ_b and is calculated using Equation 1.1. The helix angle at the barrel wall for a square-pitched screw is 17.7°.

$$\tan\theta_b = \frac{L}{\pi D_b} \quad \text{thus} \quad \theta_b = \arctan\frac{L}{\pi D_b} \tag{1.1}$$

The relationship between the width of the channel perpendicular to the flight at the barrel interface, W_b, and the axial distance between the flight edges at the barrel interface, B_b, is as follows:

$$W_b = B_b\cos\theta_b = \left(\frac{L}{p} - b_b\right)\cos\theta_b = \frac{L}{p}\cos\theta_b - e \tag{1.2}$$

$$e = b_b\cos\theta_b \tag{1.3}$$

As mentioned earlier, several of the geometric parameters are a function of the radial position (r) of the screw. These parameters include the helix angle and the channel widths. The length of an arc for one full turn at the barrel surface is πD_b. At the screw surface the length of the arc for one turn is $\pi(D_b - 2H)$; the lead length, however, remains the same. This leads to a larger helix angle at the screw root than at the barrel surface. This analysis is for a flight width that does not change with the depth of channel. As discussed in Chapter 10, for a properly designed screw, the flight width will increase as the root of the screw is approached due to the flight radii.

The helix angle and the channel widths at the screw core or root are designated with a subscript c, and they are calculated as follows:

$$\tan\theta_c = \frac{L}{\pi(D_b - 2H)} = \frac{L}{\pi D_c} \quad \text{thus} \quad \theta_c = \arctan\frac{L}{\pi D_c} \tag{1.4}$$

Thus the screw has a narrower normal distance between flights at the screw root because the helix angle is larger and because the lead remains the same.

$$W_c = B_c \cos\theta_c = \left(\frac{L}{p} - b_c\right)\cos\theta_c = \frac{L}{p}\cos\theta_c - e \tag{1.5}$$

$$e = b_c \cos\theta_c \tag{1.6}$$

For a generalized set of functions in terms of the radius, r, and the local diameter, D, the helix angle is calculated as follows:

$$\theta(r) = \arctan\frac{L}{\pi D} \tag{1.7}$$

In terms of the barrel dimensions and parameters:

$$\theta(r) = \arctan\left(\frac{D_b}{D}\tan\theta_b\right) \tag{1.8}$$

The channel width at any radius thus follows:

$$W(r) = B\cos\theta(r) = \left(\frac{L}{p} - b(r)\right)\cos\theta(r) = \frac{L}{p}\cos\theta(r) - e \tag{1.9}$$

The average channel width is used for many of the calculations in this book. This average channel width is represented as simply W here and is calculated using Equation 1.10. The use of the average channel width will be discussed in detail in Chapter 7.

$$W = \frac{W_b + W_c}{2} \tag{1.10}$$

Calculations in helical coordinates are very challenging. The procedure used in this text will be to "unwrap" the screw helix into Cartesian coordinates for the analysis. It is important to be able to calculate the helical length in the z direction at any radius r for the axial length l:

$$z(r) = \frac{l}{\sin\theta(r)} \tag{1.11}$$

1.4 Simple Flow Equations for the Metering Section

The efficient operation of a single-screw extruder requires that all three extruder sections, solids conveying, melting, and metering, must be designed to work efficiently and in coordination to have a trouble-free process. The specific analysis for each of these topics will be covered in later chapters. The simple flow calculations for the metering section should be performed at the start of any extruder troubleshooting process. It is presented at this time so that the reader may see how the equations developed in subsequent sections are used at the start of a typical troubleshooting problem.

For a properly operating smooth-bore single-screw extruder, the metering section of the screw must be the rate-limiting step of the process. Thus, calculation of the flows in the metering section of a process can be used to determine if the extruder is operating properly. A simple and fast method of estimating the flow components in a metering section was developed by Rowell and Finlayson [5] for screw pumps, and it was outlined in the Lagrangian frame by Tadmor and Klein [4]. These flows are based on a reference frame where the barrel is rotated in the opposite direction from the normal screw rotation, and they are historically called drag flow and pressure flow. Screw rotation analysis, as developed by Campbell and coworkers [6 – 15], is used here to arrive at the same flow equations while retaining the screw rotation physics of the extruder. For screw rotation, the flows are called rotational flow and pressure flow. This screw rotation analysis has been shown to provide a better understanding of the flow mechanism in the extruder, a better estimate of viscous dissipation and temperature increase in the extruder, and a better prediction of the melting characteristics. Several other methods are available for estimating the flow components in the metering section of a screw, but they can be more complicated and time consuming [16].

The method described here is the simplest of all methods. This simplicity is based on numerous assumptions (listed below), and thus it requires a minimum amount of data and computational effort. The calculation is only meant to give a quick and crude estimate of the flows, since in most cases assumptions 4 through 7 are violated. An improved yet more difficult method is introduced in Chapter 7. The assumptions for the simple calculation method are as follows:

1. Flow is fully developed.
2. Flow channels are completely filled.
3. No slip at the boundary surfaces.
4. No leakage flow over the flight tips.
5. All channel corners are square.

6. Flows are isothermal and Newtonian.
7. Channel dimensions are not changing in the metering section.

The fully developed flow components in a constant-depth metering section can be estimated using flow analysis for a long rectangular channel, as outlined in Chapter 7. For those calculations, a geometry transformation is first performed. That is, the channels of the screw are "unwound from the helix" and "straightened into a long trough." The barrel now becomes an infinitely large flat plate. Next, the screw or trough is moved at a fixed angle to the stationary barrel. These equations were developed using a Cartesian coordinate system; that is, the z direction is in the down-channel direction and parallel to the flight edge, the y direction is normal to the barrel surface, and x is the cross-channel direction and thus perpendicular to the flight edge.

The geometric parameters for a screw in the "wound" form are shown by Figure 1.5 for a single-flighted screw.

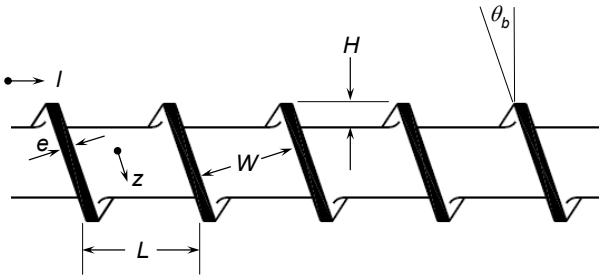

Figure 1.5 Geometric parameters for a single-flighted screw in the wound state

Two driving forces for flow exist in the metering section of the screw. The first flow is due just to the rotation of the screw and is referred to as the rotational flow component. The second component of flow is due to the pressure gradient that exist in the z direction, and it is referred to as pressure flow. The sum of the two flows must be equal to the overall flow rate. The overall flow rate, Q, the rotational flow, Q_d, and the pressure flow, Q_p, for a constant depth metering channel are related as shown in Equation 1.12. The subscript d is maintained in the nomenclature for historical consistency even though the term is for screw rotational flow rather than the historical drag flow concept.

$$Q = Q_d - Q_p \tag{1.12}$$

The volumetric rotational flow term (Q_d) depends on the several geometric parameters and rotation speed. Since most extruder rates are measured in mass per unit time, the term Q_{md} is defined as the mass rotational flow:

$$Q_d = \frac{pV_{bz}WHF_d}{2} \tag{1.13}$$

$$Q_{md} = \frac{p\rho_m V_{bz} WHF_d}{2} \tag{1.14}$$

where ρ_m is the melt density at the average fluid temperature of the resin, V_{bz} is the z component of the screw velocity at the barrel wall, H is the depth of the channel, and F_d is the shape factor for plane Couette flow. The analysis using plane Couette flow does not take into account the effect of the flights (channel helix) on the flow rate. The F_d term compensates for the reduction in flow rate due to the drag-induced resistance of the flights. For an infinitely wide channel with no flights, F_d would be equal to 1. As the channel width approaches the depth, F_d is about 0.5.

The analysis developed here is based on screw rotation physics [13], and thus several other definitions are developed here. The velocities at the screw core, indicated by the subscript c, in the x and z directions are as follows:

$$V_{cx} = \pi N D_c \sin\theta_c \tag{1.15}$$

$$V_{cz} = -\pi N D_c \cos\theta_c \tag{1.16}$$

where N is the screw rotation rate in revolutions per second. Cross-channel velocity for the screw in the laboratory frame (screw rotation frame) is

$$V_x = V_{cx}\left(1+\frac{H}{R_c}\right)\frac{y}{H}\left(2-3\frac{y}{H}\right)+V_{cx}\left(1+\frac{y}{R_c}\right) \tag{1.17}$$

where R_c is the screw core radius.

The down-channel velocity in the laboratory frame for very wide channels ($H/W < 0.1$) as a function of the height of the channel y is as follows:

$$V_{dz} = \frac{y}{H}|V_{cz}|\left(1+\frac{H}{R_c}\right)-|V_{cz}|\left(1+\frac{y}{R_c}\right) \tag{1.18}$$

Pressure flow velocity in the z direction for a very wide channel ($H/W < 0.1$) as a function of y is

$$V_{pz} = \frac{H^2}{8\eta}\frac{\partial P}{\partial z}\left[\left(\frac{y}{H}\right)^2-\frac{y}{H}\right] \tag{1.19}$$

The z component of the screw velocity at distance H from the screw root is computed as

$$V_{bz} = \pi N D_b \cos\theta_b \tag{1.20}$$

or

$$V_{bz} = V_{cz}\left(1+\frac{H}{R_c}\right) \tag{1.21}$$

The volumetric pressure flow term, Q_p, and the mass flow pressure flow term, Q_{mp}, are computed as follows:

$$Q_p = \frac{pWH^3F_p}{12\eta}\left[\frac{\partial P}{\partial z}\right] \tag{1.22}$$

$$Q_{mp} = \frac{p\rho_m WH^3F_p}{12\eta}\left[\frac{\partial P}{\partial z}\right] \tag{1.23}$$

where F_p is the shape factor for pressure flow, $\partial P / \partial z$ is the pressure gradient in the channel in the z direction, and η is the shear viscosity of the molten polymer at the average channel temperature and at an average shear rate, $\dot{\gamma}$:

$$\dot{\gamma} = \frac{\pi D_c N}{H} \tag{1.24}$$

The shear rate in the channel contains contributions from the rotational motion of the screw and the pressure-driven flow. The calculation of the shear rate, $\dot{\gamma}$, using Equation 1.24, is based on the rotational component only and ignores the smaller contribution due to pressure flow. For the calculations here, Equation 1.24 can be used.

The relationship between the pressure gradient in the z direction to the axial direction, l, is as follows:

$$\frac{\partial P}{\partial z} = \frac{\partial P}{\partial l}\sin\theta_b \tag{1.25}$$

The pressure gradient is generally unknown, but the maximum that it can be for a single-stage extruder screw is simply the discharge pressure, P_{dis}, divided by the helical length of the metering section. This maximum gradient assumes that the pressure at the start of the metering section is zero. For a properly designed process, the actual gradient will be less than this maximum, and the pressure at the start of the metering section will not be zero.

$$\frac{\partial P}{\partial z} = \frac{P_{dis}\sin\theta_b}{l_m} \tag{1.26}$$

where l_m is the axial length of the metering section. The shape factors F_d and F_p [4, 17] are computed to adjust for the end effect of the flights. The factors are from the summation of an infinite series as part of an exact solution for the constant temperature and constant viscosity solution in the z direction in the unwound screw channel. The factors are calculated as follows:

$$F_d = \frac{16W}{\pi^3 H} \sum_{i=1,3,5,\ldots}^{\infty} \frac{1}{i^3} \tanh\left(\frac{i\pi H}{2W}\right) \tag{1.27}$$

$$F_p = 1 - \frac{192H}{\pi^5 W} \sum_{i=1,3,5,\ldots}^{\infty} \frac{1}{i^5} \tanh\left(\frac{i\pi W}{2H}\right) \tag{1.28}$$

The shape factors range from 0 to 1 and approach 1 for shallow channels; that is, $H / W \approx 0$. It is important to include the shape factors when evaluating commercial screw channels. This becomes extremely important for deep channels where H/W does not approach 0. The total mass flow rate, Q_m, is calculated by combining the flow components as provided in Equation 1.29 for the total mass flow rate. As stated previously, the rate, rotational flow, and pressure flow calculations should be performed at the start of every troubleshooting project.

$$Q_m = \frac{p\rho V_{bz} WHF_d}{2} - \frac{p\rho WH^3 F_p}{12\eta}\left[\frac{\partial P}{\partial z}\right] \tag{1.29}$$

1.5 Example Calculations

Three examples are presented that introduce the use of the equations developed in this chapter. These calculations should be used at the start of the performance analysis of all troubleshooting problems. This analysis will be expanded in subsequent chapters through Chapter 7 using additional tools and understandings to complete the troubleshooting process.

1.5.1 Example 1: Calculation of Rotational and Pressure Flow Components

A manager decided to buy a new 88.9 mm (3.5 inch) diameter general purpose extruder to extrude products using several different low-density polyethylene (LDPE) resins. The die manufacturer has indicated that the die entry pressure will be 12.4 MPa. Both vendors used nominal viscosity data for a commercial LDPE resin at a temperature of 210 °C when doing their predictions because the manager had not yet settled on the resins or manufacturer for the new materials. The manager has specified that the extruder must be capable of running flood-fed at a maximum rate of 250 kg/h. Flood feeding refers to the operation of the extruder with resin covering the screw in the feed hopper. In this operation, increasing the screw speed will increase the rate of the process. The shear viscosity specified was

2000 Pa·s. The melt density for LDPE resin at 210 °C is 0.75 g/cm^3. The screw was specified with a 6 diameter long feed section with a constant channel depth of 16.51 mm, a 9 diameter long transition section, and a 9 diameter long metering section with a constant channel depth of 5.08 mm. The screw lead length is 1.2 times the screw diameter at 107 mm and the screw flight width perpendicular to the flight edge is 9.0 mm. The extruder manufacturer has stated that the extruder is capable of a maximum screw speed of 108 rpm. Will this extruder meet the desired rate expectations of the manager for the LDPE resin?

In order to address this key question, the information provided in this chapter will be used to calculate the geometrical and flow data for this analysis. When making the calculations for any engineering analysis it is absolutely imperative that the same units system be used for all the calculations. It is generally accepted today that the calculations are performed using the SI units system [18]: mass in kilograms, length in meters or some fraction thereof, time in seconds, energy in joules, pressure in Pascal, and viscosity in Pascal seconds.

To start the calculation, the geometrical parameters are calculated based on the known specifications for the metering channel of the screw. Only the metering channel is considered here since the metering channel is the rate-controlling operation for a properly designed screw and a smooth-bore extrusion process. The specifications and calculated values for the metering channel of the screw are provided in Table 1.1 along with the equations used for the calculations.

Table 1.1 Geometric Parameter Values for the Screw in Example 1

Parameter	Value	Equation
Barrel diameter, D_b	88.9 mm	
Core diameter, D_c	78.74 mm	
Lead length, L	107 mm	
Meter channel depth, H	5.08 mm	
Flight width, e	9.0 mm	
Flight starts, p	1	
Helix angle at the barrel, θ_b	21.0°	1.1
Helix angle at the screw core, θ_c	23.4°	1.4
Channel width at the barrel, W_b	90.9 mm	1.2
Channel width at the screw core, W_c	89.2 mm	1.5
Average channel width, W	90.0 mm	1.10
Channel aspect ratio, H/W	0.056	
Unwrapped channel length for one turn, z_b	299 mm	1.11
Total helical length of the metering section, Z_b	2.23 m	1.11
Shape factor for rotational flow, F_d	0.966	1.27
Shape factor for pressure flow, F_p	0.965	1.28

Since the manager is asking for an extruder and screw that will provide 250 kg/h, the expected maximum rate will be calculated at the maximum screw speed of 108 rpm. At a screw speed of 108 rpm (N = 1.80 rev/s), the z component of the flight tip velocity (V_{bz}) at H is calculated at 469 mm/s using Equation 1.20. Now all terms required to calculate the rotational mass flow rate are known and are calculated using Equation 1.14:

$$Q_{md} = \frac{(750\ \text{kg/m}^3)(0.469\ \text{m/s})(0.090\ \text{m})(5.08\times10^{-3}\ \text{m})(0.966)}{2}$$
$$= 0.077\ \text{kg/s} => 280\ \text{kg/h}$$

For this calculation, the density of the molten LDPE resin is known to be 750 kg/m^3 at 210 °C. Next, the pressure flow term needs to be calculated based on the maximum pressure gradient possible in the metering channel. The maximum pressure gradient will occur when the pressure at the entry to the metering section is near zero. In practice, the pressure at the entry to the meter will be considerably higher. With zero pressure at the entry and 12.4 MPa at the discharge (die entry pressure), the maximum pressure gradient is estimated by dividing the pressure change by the helical length (Z_b) of the metering channel. This maximum pressure gradient $\partial P / \partial z$ is calculated at 5.56 MPa/m. Since the pressure is increasing in the helical direction, the pressure gradient is positive. Next, the mass flow rate due to the pressure gradient is calculated using Equation 1.23 and a shear viscosity of 2000 Pa·s as follows:

$$Q_{mp} = \frac{(750\ \text{kg/m}^3)(0.090\ \text{m})(5.08\times10^{-3}\ \text{m})^3(0.965)}{12(2000\ \text{Pa}\cdot\text{s})}\left(\frac{5.56\times10^{6}\ \text{Pa}}{\text{m}}\right)$$
$$= 0.0020\ \text{kg/s} => 7\ \text{kg/h}$$

The overall mass rate expected from the extruder and screw specification was calculated using Equation 1.12 at 273 kg/h. The manager specified a rate of 250 kg/h for the process. Since the extruder is capable of 273 kg/h at the maximum screw speed, the extruder is specified properly from a rate viewpoint. Further calculations indicated that 250 kg/h of LDPE could be extruded at a screw speed of 99 rpm for a maximum pressure gradient of 5.56 MPa/m, discharging at 210 °C and a pressure of 12.4 MPa. The pressure mass flow Q_{mp} is very low, at about 2% of the rotational mass flow Q_{md}. If the screw geometry is kept constant, this ratio will increase if the discharge pressure increases or the viscosity decreases. As this book progresses, the solution for Example 1 will be expanded as new materials are introduced in subsequent chapters through Chapter 7.

1.5.2 Example 2: Flow Calculations for a Properly Operating Extruder

For this example, a plant is using a smooth-bore extruder to process an LDPE resin. At a screw speed of 100 rpm, the extruder is operating flood-fed with a rate of 800 kg/h. For these conditions, the plant personnel have measured the discharge pressure at 15.9 MPa and the discharge temperature at 210 °C. The plant manager wants to know if this extruder is operating properly and whether the metering section of the screw is controlling the rate. For this case, the extruder is 152.4 mm in diameter, D_b, the lead length, L, is 152.4 mm, the width of the flight, e, is 15.2 mm, and the channel depth, H, in the metering section is 6.86 mm. The metering section length is 76.2 cm or 5 turns. The melt density for LDPE resin at 210 °C is 0.750 g/cm^3.

The shear rate for this example is estimated using Equation 1.24 to be 106 1/s. The viscosity for this LDPE resin at 210 °C and a shear rate of 106 1/s is about 300 Pa·s. From the screw geometry, screw speed, and melt density, the rotational flow rate, Q_{md}, is computed at 888 kg/h. Since the rotational flow and pressure flow must equate to the total flow using Equation 1.29, the pressure flow rate, Q_{mp}, is 88 kg/h. The positive sign for the pressure flow rate term means that the pressure gradient is reducing the flow. Likewise, a negative pressure flow rate term would mean that the pressure gradient is causing the flow rate to be higher than the rotational flow rate. For this resin and a viscosity of 300 Pa·s, the pressure gradient in the channel is calculated using Equation 1.29 as 1.40 MPa/turn. Thus, the discharge end of the metering channel is at a higher pressure than the entry.

To answer the question as to whether the extruder is operating properly, several additional calculations are performed. For this screw, there are 5 screw turns in the metering section, which is calculated by dividing the axial length (76.2 cm) by the lead length (L = 152.4 mm). Multiplying the number of turns by the pressure gradient in the metering section reveals that the total pressure increase in the metering section is 7.0 MPa. To achieve the measured discharge pressure of 15.9 MPa, the pressure at the entry of the metering section must be 8.9 MPa. Because a positive pressure over the entire length of the metering section is occurring, the calculations indicate that the screw is full with resin and functioning properly. That is, the metering section is controlling the rate. The axial pressure profile for this case is shown in Figure 1.6.

1.5.3 Example 3: Flow Calculations for an Improperly Operating Extruder

An extruder with a metering section having the same geometry as the extruder in Example 2 is operating flood-fed at a rate of 550 kg/h. The screw speed is 100 rpm, the discharge temperature is 210 °C, and the discharge pressure is 10.3 MPa. Is this extruder operating properly so that its metering section is controlling the

rate? Because the metering section geometry, screw speed, and discharge temperature have not changed, the method still calculates the rotational flow rate component as 888 kg/h. However, the pressure flow component is now calculated as 338 kg/h, and the pressure gradient corresponding to this flow is 5.4 MPa/turn. To determine if the extruder is operating properly, the pressure generating capacity needs to be calculated by multiplying the 5 screw turns in the metering section length by the pressure gradient. The result is a total pressure increase of 27 MPa in the metering section. This pressure increase is greater than the 10.3 MPa pressure measured at the discharge of the extruder. In fact, only 1.9 diameters of the metering section length are required to generate a discharge pressure of 10.3 MPa (calculated by dividing 10.3 MPa by 5.4 MPa/turn). This means that the remaining 3.1 diameters of the metering section are at zero pressure and are only partially filled. A partially filled system will always be at zero pressure. Because a positive pressure over the entire length of the metering section is not possible, the calculations indicate that the metering section is not full and is not functioning properly. A process upstream of the metering section is controlling the rate.

Figure 1.6 shows the axial pressures for the extruders described in Examples 2 and 3. In this figure, the solid lines were calculated while the dotted lines were estimated based on experience. For Example 2, where the extruder operates properly, the extruder pressure is positive at all axial positions. Thus, all the channel sections are operating full and under pressure as designed. For Example 3, where the extruder operates improperly, the extruder pressure is zero for portions of the melting and metering sections. In these portions of the extruder, the screw channel is not pressurized, and the extruder is operating partially filled. This means that the metering section is not controlling the rate as designed, and the screw is not operating properly. Extruders that are operated partially filled in the metering section can have low production rates, high scrap rates, and material degradation, and cause high labor costs.

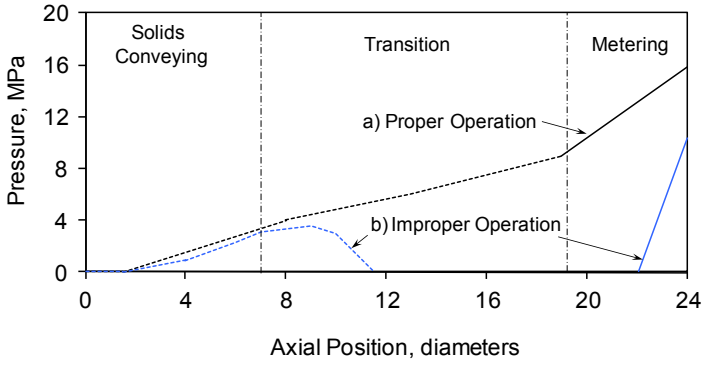

Figure 1.6 Axial pressure profiles for a) Example 2 where the extruder is operating properly (all channels are full and pressurized), and b) Example 3 where the extruder is operating improperly. For Example 3, the channel is not pressurized between diameters 12 and 22, indicating that the channels are partially filled at these locations

1.5.4 Metering Channel Calculation Summary

Calculation of the rotational flow rate and an estimate of the pressure profile in the metering channel should be performed for all design and troubleshooting projects. As shown in the example problems, the rate can be quickly and easily estimated for a new installation. The calculation method should always be performed for machines that are operating at low rates and have degradation products in the extrudate. As described in Section 1.5.3, the calculation is capable of predicting partially filled channels in the metering section. Partially filled metering channels will cause the resin to degrade, and the degradation products will eventually be discharged from the machine, contaminating the final product.

Nomenclature

b_b axial flight width at the barrel wall

b_c axial flight width at the screw root

B axial channel width as a function of the radial position

B_b axial channel width at the barrel wall

B_c axial channel width at the screw core

D local diameter

D_b inner diameter of the barrel

D_c diameter of the screw core

e flight width of the screw and perpendicular to the flight edge

F_d shape factor for rotational flow

F_p shape factor for pressure flow

H local distance from the screw root to the barrel

l axial distance

l_m axial distance for the metering section

L lead length

N screw rotation speed in revolutions/s

p number of flight starts

P_{dis} discharge pressure

P pressure in the channel

Q volumetric flow rate

Q_d volumetric rotational flow rate

Q_m mass flow rate

Q_{md} mass rotational flow rate

Q_{mp} pressure-induced mass flow rate

Q_p volumetric pressure flow rate

R_c radius of the screw core

V_{dz} down-channel velocity (z direction) as a function of y

V_{pz} z component of the velocity due to a pressure gradient

V_x cross-channel velocity (x direction) in the channel as a function of y

V_{cx} x component of velocity of the screw core

V_{cz} z component of velocity of the screw core

V_{bz} z component of velocity of the screw flight at the barrel wall

W average channel width

W_b channel width perpendicular to flight at the barrel wall

W_c channel width perpendicular to flight at the screw core

$W(r)$ channel width perpendicular to flight at radius r

x independent variable for the cross-channel direction perpendicular to the flight edge

y independent variable for the direction normal to the barrel surface (channel depth direction)

z independent variable in the down-channel direction (or helical direction)

z_b helical length of the channel at the barrel wall

$z(r)$ helical length of the channel at radial position r

Z_b helical length of the metering channel at the barrel wall

$\dot{\gamma}$ average shear rate in the channel

η shear viscosity of the polymer at the average channel temperature and average shear rate, $\dot{\gamma}$

θ_b helix angle at the barrel

θ_c helix angle at the screw core

$\theta(r)$ helix angle at radial position r

λ mechanical clearance between the top of the screw flight and the barrel wall

ρ_m melt density of the fluid

References

1. Kamal, M. R., Isayev, A. I., and Liu, S-J., "Injection Molding Technology and Fundamentals," Hanser Publications, Munich (2009)
2. Kirkland, C., "Damage Control Saturn Style," *Injection Molding Magazine*, September (1994)
3. Chung, C. I. and Barr, R. A., "Energy Efficient Extruder Screw," U. S. Patent 4, 405, 239 (1983)
4. Tadmor, Z. and Klein, I., "Engineering Principles of Plasticating Extrusion," Van Nostrand Reinhold Co., New York (1970)
5. Rowell, H. S. and Finlayson, D., "Screw Viscosity Pumps," *Engineering*, **114**, 606 (1922)
6. Campbell, G. A., Tang, Z., Wang, C., and Bullwinkel, M., "Some New Observations Regarding Melting in Single Screw Extruders," *SPE ANTEC Tech. Papers*, **49**, 213 (2003)
7. Campbell, G. A. and Tang, Z., "Solid Bed Melting in Single Screw Extruders – An Alternative First Order Mechanism," *SPE ANTEC Tech. Papers*, **50**, 162 (2004)
8. Campbell, G. A. Wang, C., Cheng, H., Bullwinkel, M., and te-Riele, M. A., "Investigation of Flow Rate and Viscous Dissipation in a Single Screw Pump-Extruder," *Int. Polym. Process.*, **16**, 323 (2001)
9. Campbell, G. A. and Dontula, N., "Solids Transport in Extruders," *Int. Polym. Process.*, **10**, 30 (1995)
10. Campbell, G. A., Spalding, M. A., and Carlson, F., "Prediction of Screw Temperature Rise in Single Screw-Pump Extruders," *SPE ANTEC Tech. Papers*, **54**, 267 (2008)
11. Campbell, G. A., Sweeney, P. A., and Felton, J. N., "Experimental Investigation of the Drag Flow Assumption in Extruder Analysis," *Polym. Eng. Sci.*, **32**, 1765 (1992)
12. Campbell, G. A., Sweeney, P. A., and Felton, J. N., "Analysis of an Alternative Extruder Screw Pump Design," *Int. Polym. Process.*, **7**, 320 (1992)
13. Campbell, G. A., Sweeney, P. A., Dontula, N., and Wang, Ch., "Frame Indifference: Fluid Flow in Single Screw Pumps and Extruders," *Int. Polym. Process.*, **11**, 199 (1996)
14. Campbell, G. A., Cheng, H., Wang, C., Bullwinkel, M., and te-Riele, M. A., "Temperature Rise in a Single Screw Pump-Extruder," *SPE ANTEC Tech. Papers*, **47**,152 (2001)
15. Campbell, G. A., Spalding, M. A., and Tang, Z., "An Alternative Analysis of Single-Screw Melting," *SPE ANTEC Tech. Papers*, **55**, 147 (2009)
16. Spalding, M. A., Dooley, J., Hyun, K.S, and Strand, S. R., "Three Dimensional Numerical Analysis of a Single-Screw Extruder, " *SPE ANTEC Tech. Papers*, **39**, 1533 (1993)
17. Squires, P. H., "Screw Extruder Pumping Efficiency," *SPE J.*, **14**, 24 (1958)
18. Conant, F. S., "Using the SI Units," *Polym. Eng. Sci.*, **17**, 222 (1977)

2 Polymer Materials

A brief discussion of polymer materials is presented here to introduce the extrusion practitioner to material properties and how they relate to extrusion and polymer processing. The discussion presented here is intended to introduce several characteristics of polymer materials that can be affected during processing using single-screw extruders. For example, different in-specification lots of the same resin may vary slightly in molecular weight and thus can require different power levels to extrude. Moreover, poorly designed extrusion systems can cause the polymer to degrade in the extruder, leading to black specks in a product. Styrenic resins can degrade to produce a styrene odor at the die, especially at high processing temperatures. Other materials such as polyester resins and polyurethane elastomers can have reduced mechanical properties if they are improperly extruded. Clearly, the design of a high-performance extrusion process is highly dependent on the characteristics of the materials processed.

This chapter will introduce a brief history of polymers, the structure of polymers, and several methods for classifying and quantifying their properties from a molecular and a macroscopic point of view. The general concept of what constitutes a polymer will be introduced, including the molecular characteristics of polymers that control viscous flow and the mechanical properties. The chapter also introduces the chemical reactions for producing polymers and the degradation reactions that commonly occur in an extruder. Polymer rheology and viscoelasticity will be presented in Chapter 3. Other physical properties related to processing are presented in Chapter 4. All of these properties are related to the polymer structure and strongly affect the extrusion and mixing of polymers.

2.1 Introduction and History

Polymers are a class of materials that have large molecules made up of many repeating units or mers. The relationship between a mer and polymers will become clearer as this chapter progresses. All synthetic polymers are macromolecules that are made from as many as 20,000 mers in each molecule. The reactant is typically only one mer and is thus referred to as the monomer. Some natural polymers have many more mers per molecule, such as natural rubber with a molecular weight of over 1 million kg/kg-mol when removed from the rubber tree. Inorganic polymers are an interesting subset of synthetic polymers. Polyphosphates, polysilicates, and polysilicones are classes of inorganic polymers that have substantial commercial interest as ion exchange resins, surfactants, and coatings. Inorganic polymers are generally not extruded, so they will not be discussed further in this book. Polymers of interest here are primarily composed of carbon, oxygen, nitrogen, and hydrogen, although other atoms can occur. These organic polymers are all macromolecules. Natural polymers are formed from peptide molecules, resulting in polypeptide polymers. The polypeptide repeating unit is shown in Figure 2.1. These polymers are found in animal hooves, skin, hair, tendons, and proteins. Although these polymers function well for the organism, their utility as commercial polymers is limited by their lack of diversity in properties, especially mechanical properties.

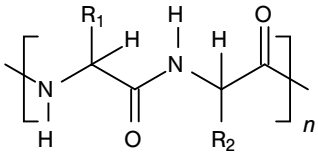

Figure 2.1 Chemical structure of polypeptides. The R_1 and R_2 group possibilities are shown in Figure 2.2, and *n* is the number of repeating units in the molecule

There has been a tremendous interest in polymers since World War II. In the US, consumption was 18 million metric tons in 1974, 25.7 million metric tons in 1984, and 41.3 million metric tons in 1994 [1]. Polymer production has increased from essentially zero at the end the World War II to about 101 million metric tons worldwide in 1993 [2] and 241 million metric tons in 2006 [3]. The reason for this increase is quite simple. Synthetic polymers are numerous in structure and are very diverse in their structure-property relationships. Polymers are used extensively in electrical applications, including insulators, capacitors, and conductors. They are also used in many optical applications, the biochemical industry, structural applications, packaging, and they are used extensively as thermal insulation [4].

2.1.1 History of Natural Polymers

Natural polymers have been used by humans since the dawn of history and civilization. Natural polymers have been used by early humans for making tools, weapons, clothing, shelter, and sporting objects. Many natural polymers came from the animals that were either hunted or domesticated. Our ancestors used the skin, bone, and horn in their daily existence. The Mayans used a rubber ball of coagulated latex in their national sport. As an incentive to play at peak performance, the Mayans would kill the losing team. Today, many natural polymers are used commercially, including wood, rubber, silk, cotton, leather, paper, oil-based paints, and casein (adhesives). Moreover, many active industrial programs are focused on making environmentally friendly polymers from starch [5, 6], cellulose, and lactic acid derived from plant sugar or corn. Lactic acid is then converted to polylactic acid (PLA) [7].

As expected, the mechanical properties of polymers are their most-utilized characteristic. Polymers play a very strong functional role in animals, and as indicated above these polymers are all polypeptides. The structure of these polymers is such that they have "backbone" repeating units that can be considered to be their mers. The term backbone is commonly used to describe the longest section of the polymer. All of these polypeptides have two side-chain groups on the mer, designated as R_1 and R_2. Several side groups are shown in Figure 2.2. These side groups can be neutral, negatively charged, or positively charged. The counter ions for the negatively charged group include Na^+ and K^+ while the counter ions for the positively charged group include Cl–. Other counter ions are known to exist.

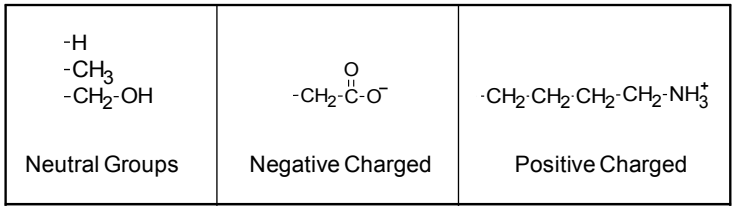

Figure 2.2 Several side groups for polypeptides

The side groups and the repeating structure of the side groups change the chemical and physical properties of the polymer, and this defines the chemical and physical characteristics of the different polypeptide molecules. Not all natural macromolecules, however, are polymers. For example, insulin is a natural macromolecule with a molecular weight of 5733 kg/kg-mol. Insulin has long linear chains that are connected by 21 sulfur crosslinks. When it is decomposed 51 residual molecules result. Insulin is not a polymer because it does not have repeating units of monomers.

Another important class of natural polymers is polysaccharides. The two most common are cellulose and starch. Cellulose has a molecular weight greater than 1 million kg/kg-mol while starch has a very similar structure but a molecular weight of only 10,000 to 40,000 kg/kg-mol. Cellulose comes from woody plants and represents about 50% of the plant mass. Cellulose is the material in pulp fibers that constitutes the paper in this book. The other half of the woody material is lignin. The lignin holds the cellulose together, and it is discarded in the pulping process. It is interesting to note that the structure of lignin has not been quantified. This is because it has to be chemically destroyed to remove it from the wood to obtain the cellulose. The chemical process of removing lignin alters the molecule in such a random way that the molecular structure of the original molecule has yet to be confirmed. The dominant commercial chemical that has been produced economically from lignin is synthetic vanilla for flavoring foods. Early manufacturing plants used the sulfite process to separate the cellulose from the lignin, and the lignin with large volumes of water was discharged into rivers. With the advent of the environmental movement the paper industry moved away from the sulfite process and has moved to a great extent to the Kraft pulping process [8]. This process is characterized by an organic sulfur odor in the vicinity of many current pulp mills. The reason that this process has become economically important is that the lignin spent liquor can be concentrated and burned to recover its energy. Cellulose is an important starting material for a number of commercial polymers, including cellulose acetate (rayon) fibers and composites [9, 10].

From an end-use point of view, natural polymers have consistent properties, but they lack diversity. That is, these polymers provide the consistent properties required by the organism. Many new commercial applications, however, were identified that could not be met by natural polymers, creating the need to develop a large number of synthetic polymers. By changing the chemistry, synthetic polymers can be made that are hard-glassy resins, soft-sticky adhesives, strong-tough textile fibers, highly extensive elastomers, and durable surface coatings.

2.1.2 The History of Synthetic Polymers

Some important everyday items that are made from polymers with widely different properties include billiard balls, plastic dishes, soda bottles, barrier and decorative films, egg cartons, polymeric drinking glasses, foam seats, and automotive tires. These applications for synthetic polymers have developed over about 150 years. As shown in Table 2.1, modern polymer material science and technology can be traced back to as early as 1770 [1]. Some important advances in the understanding of polymer production were developed before World War II.

Table 2.1 Important Dates for Development or Implementation of Polymeric Materials before World War II [1]

Year	Advancement
1770	Priestly is said to have given rubber its name because it erased pencil marks.
1838	Regnault polymerized vinylidene chloride (PVDC) using sunlight.
1839	Discovery of the vulcanization of rubber.
1868	Hyatt produced billiard balls from cellulose nitrate.
1907	Baekeland developed phenol-formaldehyde resin.
1910	First rayon plant built in the US.
1929	Carothers produced condensation polymers.
1930s	Development of polychloroprene, PMMA, PS, PA 66, PVDC.

In 1838 Macintosh and Hancock at Goodyear discovered how to take tacky natural rubber from rubber trees and react it with sulfur in the presence of heat to vulcanize the rubber to a nonstick compound that could be useful for items such as boots, rain coats, and tires. Synthetic rubber research started between World Wars I and II and progressed very quickly after World War II. The modern birth of solid synthetic polymers for commercial products may be traced to Hyatt in 1868. He discovered how to react cellulose nitrate and camphor to produce a hard plastic that was used to fabricate billiard balls because ivory had become scarce.

The growth in polymer science and technology was accelerated dramatically during and since World War II. For example, the understanding of science and engineering of synthetic polymers dramatically accelerated during World War II because of the GR-S (government rubber styrene) SBR (styrene-butadiene rubber) project. The GR-S project was a huge project initiated by the US government and industrial partners to develop SBR materials [11]. At the start of this project the US was not producing synthetic rubber, and all rubber articles were based on natural rubber. A maritime blockade by Japan during World War II caused the loss of access to natural latex and rubber from Asia. In 1940 the US produced no synthetic rubber. By the year 1945 the US was producing 700,000 tons per year of SBR. The military vehicles used during World War II needed to have rubber tires that would work in both hot and very cold environments. This war-driven project had a much more important influence on the polymer industry than just the production of synthetic rubber. More importantly the project trained people, provided insight into polymer characterization, and developed an understanding of the engineering necessary to purify and transport monomers and build production facilities. The development of polymer science and technology accelerated after World War II, as shown in Table 2.2.

Table 2.2 Important Dates for Development or Implementation of Polymeric Materials after World War II [1]

Year	Advancement
1945	Cellulose propionate
1946	Screw injection molding
1947	Epoxy resins
1948	ABS resins
1948–1950	Acrylic fibers
1949	Blow molding
1950	Ziegler and Natta developed vinyl polymers; Swarc developed living polymers
1954	Polyurethane foam in the US; SAN copolymers
1958	Rotational molding
1960	Spandex developed by Shivers
1962	Phenoxy resins; polyimide resins
1970s	Polybutene resins; reaction injection molding; interpenetrating networks; polyester beverage bottles; aromatic polyamides; UNIPOL™ gas phase polymerization process; LLDPE resins
1980s	Polysilanes; liquid crystalline polymers; poly(etheretherketone); conducting polymers; polyetherimide
1990s	Metallocene catalysts and resins; living cationic polymerization; syndiotactic polystyrene commercialized; styrene-ethylene copolymers; nanocomposites
2000s	Olefinic block copolymers (OBC) [12]

UNIPOL™ is a trademark of Univation Technologies, LLC

2.2 Characteristics of Synthetic Polymers

This introductory section develops some of the organic and physical chemistry of polymeric materials. The discussion is approached from the viewpoint of a process engineer's needs and thus does not use a fundamental chemistry mechanistic approach. With this approach, atoms can be considered to be spherical structures, with a very dense core of protons and neutrons, and a large fraction of unfilled space defined by the electron cloud. Around this dense core the atom's electrons rotate at several average distances called orbitals. The electrons in the outer orbital shell are called the valence electrons. Generally it is accepted that atoms bond to form molecules by the interaction of the electrons in the outer orbital. One important type of bond is the ionic bond, which involves electron transfer. This type of bond is present in common table salt or sodium chloride. Typical examples of this type of bond are shown in Figure 2.3, where sodium and chlorine react to form sodium chloride and magnesium and chlorine react to form magnesium chloride.

The subscripts by the atoms in this figure are the number of electrons in the first three orbital shells, starting with the shell nearest to the nucleus. These first two shells are full and contain two and eight electrons respectively. A sodium (Na) atom has one valence electron while magnesium (Mg) and chlorine (Cl) have two and seven valence electrons, respectively. In each of these reactions, electron(s) transfer from the metal to the nonmetal, allowing chlorine to fill its outer valance shell. As a result the chlorine has a net negative charge, having one more electron than it has protons, and the sodium has a net positive charge due to having one more proton than electrons.

$$Na_{2,8,1} + Cl_{2,8,7} \rightarrow Na^{+}Cl^{-}$$

$$Mg_{2,8,2} + 2(Cl_{2,8,7}) \rightarrow Mg^{+2}(Cl^{-})_2$$

Figure 2.3 Ionic bond reactions

These ionic reactions or electron transfer reactions are not what generally occur in the structure of both natural and synthetic polymers. In polymers it is the covalent bond that dominates, and in a covalently bonded structure there is no transfer of electrons from one atom to another. Instead the electrons are shared between the adjacent atoms in the molecule. The commercial polymeric materials that will be covered in this text will generally be based on seven atomic species: silicon, hydrogen, chlorine, carbon, oxygen, nitrogen, and sulfur. Figure 2.4 shows these atoms with the number of outer valance electrons.

	**Carbon**
	**Nitrogen**
	**Silicon**
	**Oxygen**
	**Sulfur**
	**Chlorine**
	**Hydrogen**

Figure 2.4 Atoms considered when discussing polymers in this book

As indicated in Figure 2.4, all of these atoms have at least one unpaired electron in the valence or outer electron shell. A covalent bond, as suggested by the word covalent, is a bond which shares at least one pair of valence electrons between two atoms. When examining the molecular structure of polymers, it is found that all commercial polymer molecules are formed from covalent bonds.

Examination of these atoms reveals there are valence electrons numbering from one to seven in these atoms. Except for hydrogen, which has a full shell of two electrons, all of the other atoms in Figure 2.4 require eight electrons to fill the valence shell. When these shells are filled in a covalent manner by polymerization, the covalent bonds can lead to the production of large polymer molecules.

For most commercial polymers, carbon and silicon are the two backbone building blocks, and they routinely form chains of like atoms. Generally, three types of covalent bonds are associated with carbon in the production of commercial vinyl polymers, as shown in Figure 2.5: the single, double, and triple carbon-to-carbon bonds.

C:C	Single bond
C::C	Double bond
C:::C	Triple bond

Figure 2.5 Covalently bonded carbon

As stated earlier, when polymer molecules form, valence electrons are shared by the associated atoms to form covalent bonds. Carbon always has four covalent bonds, each of which is made up of two shared electrons. In Figure 2.5 the hydrogen atoms that are associated with the carbon atom in these molecules have been omitted from the diagrams. In order to meet the four covalent bond requirement, the molecule ethane must have three other covalent bonds on each carbon, and these are covalent bonds with hydrogen. These three carbon examples represent a single carbon-carbon bond for ethane, a double bond for ethylene, and a triple bond for acetylene. The single bond has two electrons, the double bond has four electrons, and the triple bond has six electrons. This leads to each carbon in ethylene having two hydrogen atoms attached, and in the case of acetylene, one covalent bonded hydrogen is attached to each carbon.

All of these chemical species have importance in the production of polymeric materials. There are several shorthand techniques for writing down the structures of polymers. The carbon-based polymer molecules using the “stick” representation are made up of atoms connected by covalent bonds (represented here by the straight lines between the carbon and the hydrogen and the carbon-to-carbon molecules), as shown in Figure 2.6. To reiterate, carbon is always tetravalent, having four covalent bonds, and a schematic of the paired electrons for two of the incorporated carbon molecules can be seen in the bottom of Figure 2.6. Thus, each “stick”

represents two electrons. For the two highlighted carbon atoms in the polyethylene molecule of Figure 2.6, the electron representation is shown, where there are four covalent bonds associated with each carbon and each bond is made up of two shared electrons represented by the black dots. This polymer molecule is made up of only carbon and hydrogen with no double bonds, and it represents a linear form of polyethylene typical of high-density polyethylene (HDPE) resin. The long chain representation of HDPE resin is shown in Figure 2.8(a). For the commercial polymers presented in this book, carbon can bond with oxygen, nitrogen, hydrogen, sulfur, chlorine, and silicon. Both carbon and silicon are chain formers while oxygen and nitrogen are typically incorporated atoms. Bonding with other atomic species, however, is possible but beyond the scope of this book. Moreover, some of these atoms have some restrictions when they react with carbon to form polymers.

a) $-CH_2-CH_2-CH_2-CH_2-CH_2-$

b) 

Figure 2.6 Representations for PE resin: a) stick method, and b) electron representation of the highlighted segment

Nitrogen and oxygen can be incorporated into the backbone such that they are surrounded by different atom types. For example, organic peroxides contain two covalently bonded oxygen atoms that form the peroxide linkage. These molecules are inherently unstable. Two covalently bonded nitrogen atoms are also similarly unstable. These unstable structures decompose to form smaller unstable molecules that are used to start the polymerization for some types of monomers. Thus, to be incorporated implies that the molecules are found only singularly in the backbone chain. Sulfur and silicon are considered to be chain formers. They can be found in the backbone in multiple units connected covalently to molecules of the same type or with carbon. Complete molecules with a silicon backbone are possible, and molecules with multiple sulfur links incorporated into the system are common, particularly in sulfur-crosslinked rubber.

■ 2.3 Structure Effects on Properties

The polymer backbone can have functional groups that are attached to some of the carbon atoms. These groups change the chemical and physical properties of the polymer molecule. If these groups are relatively short then they are usually referred to as pendant groups. Several common pendant groups are shown in Figure 2.7.

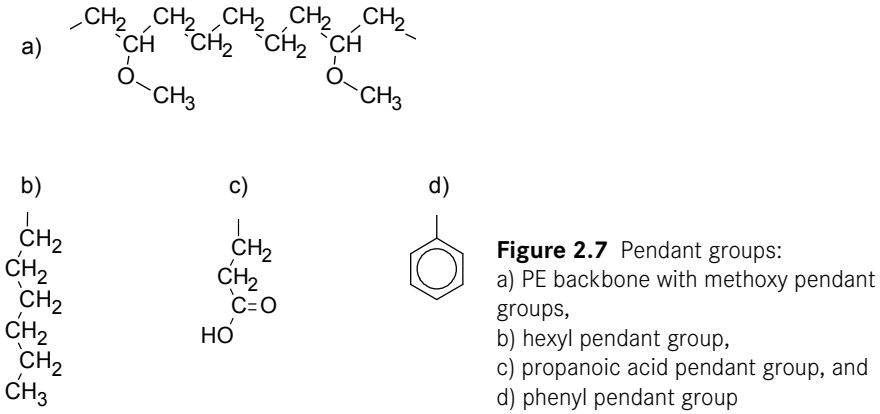

Figure 2.7 Pendant groups:
a) PE backbone with methoxy pendant groups,
b) hexyl pendant group,
c) propanoic acid pendant group, and
d) phenyl pendant group

The structure in Figure 2.7(a) shows two methoxy groups attached to the backbone of the polymer. The methoxy group consists of an oxygen atom attached to a methyl group. Another common pendant group shown is the hexyl group with six carbon atoms. The hexyl group is a prominent group in some commercial LLDPE resins, creating a level of short-chain branching as shown in Figure 2.8(b). The number of hexyl groups positioned on the backbone control the crystallinity (or solid density) and the modulus of the resin. An acid-containing group in Figure 2.7(c) is used to produce the potential for secondary reactions with inorganic salts or to form ester linkages. A phenyl group can also be a pendant group. If the phenyl group is on every other carbon then the polymer is polystyrene. Polystyrene is produced by polymerizing styrene monomer. Not shown in the figure is the CH_3 pendant group. If this group is on every other carbon atom the structure becomes polypropylene. Polypropylene is polymerized from propylene. Sometimes, pendant groups can be a large fraction of the length of the backbone. These pendant groups are then described as long-chain branches, as shown by Figure 2.8(c). Low-density polyethylene resin produced using a high-pressure reaction process has many long-chain branches. Recently, metallocene and single-site catalyst technology [13, 14] have allowed development of olefin polymers with controlled levels of long-chain branching along with short-chain branching, as depicted in Figure 2.8(d). These resins all flow when heated and are referred to as thermoplastics.

If a large number of branches exist that connect all of the backbone molecules into a three-dimensional network, the material will not flow when heated, and it is considered a thermoset resin. Vulcanized rubber is an example where the sulfur linkages create a three-dimensional network, converting the precursor rubber into a solid thermoset material. Crosslinked backbone chains are shown in Figure 2.8(e). When extruding many thermoplastics, the polymer can undergo chemical reactions to form small amounts of crosslinked material. Partial crosslinking is a problem with some PE resins that contain residual double bonds that are made using chromium catalysts. The crosslinks appear in the final product as a defect

called a gel. The catalyst residue from chromium processes can also contribute to unwanted reactions in the extrusion process [15], leading to the formation of double bonds between carbons. Moreover, crosslinking of PE resins often occurs in the extruder, especially for poorly designed processes. In polyurethanes the crosslinks can come from partial hydrolysis of the urethane bonds and then from reaction with pendant hydrogens on either the remaining urethane bonds or on polyurea bonds. PVC [16] and PVDC [17] resins undergo dehydrochlorination at elevated process temperatures, creating HCl gas, a complex mixture of hydrocarbons, and black char. Also, from an extruder troubleshooting point of view localized crosslinks can lead to gels if the crosslinking results in unmeltable structures. These structures will cause defects, including gels in extruded films or black specks in the product. These two issues will be discussed in detail in Chapter 11.

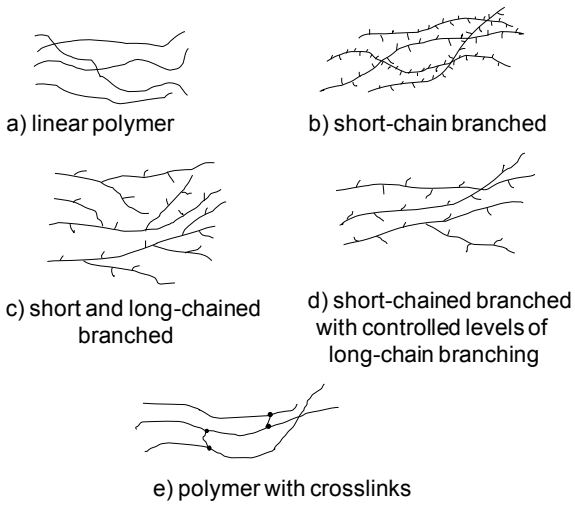

Figure 2.8 Schematic of common polymer chain structures

The straight-line representation of bond angles previously depicted is not very representative given the tetrahedral structure of carbon atoms. There is a generally accepted more stylized representation for the carbon atoms, represented in a zigzag fashion, as shown in Figure 2.9. In this representation, the hydrogen molecules are located out of the plane of the diagram. Although this comes closer to the structure of the carbon-based polymer molecule, this is still not completely representative of the structure since with single covalent bonds there is a thermal-induced rotation between the carbon bonds. These rotations at the carbon-carbon bonds control another important property of polymers, the glass transition temperature (T_g).

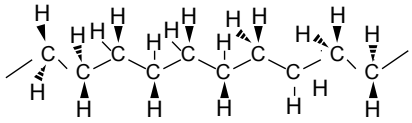

Figure 2.9 Polymer bond representations for a PE resin segment. All carbon atoms are fixed in the plane of the diagram while half of the hydrogen atoms are in front of the plane and half are behind the plane

The zigzag pattern does suggest that the carbon-carbon bond rotation must overcome a potential energy barrier to rotate around its closest carbon neighbors. This carbon-carbon backbone rotation can be strongly affected by the pendant group and by temperature, leading to different glass transition temperatures in polymer molecules.

2.3.1 Stereochemistry

Stereo structure of molecules has a strong effect on the properties and processing of materials. The concept of stereo structures is depicted in Figure 2.10 for the stereoisomers of PP where the pendant group is the methyl group. In this figure, the carbon and hydrogen atoms were omitted, and just the stick method that represents the carbon-to-carbon bonds is shown. In the case of syndiotactic polypropylene, every other methyl group is above or below the plane of symmetry; it has a melting temperature of 150 °C. In the case of isotactic polypropylene, every methyl group is on one side of the plane of symmetry. This is the form of most extrusion- and molding-grade polypropylene resins because it has the highest melting temperature of 187 °C. Finally, atactic polypropylene has the methyl groups randomly distributed above and below the plane of symmetry. This material has a glass transition temperature of –10 °C and no melting temperature. Atactic polypropylene is extensively used as a hot melt adhesive and has little or no crystalline structures. It should be emphasized that each of these different stereo structures provides very different physical properties even though the chemical structure of the monomer and polymer is the same. The different melting temperatures and properties are a result of the stereo structures of the polymers. The traditional process for making isotactic polypropylene also produces up to 20 percent atactic polypropylene, and this has to be removed before the high temperature product can be sold. Recently syndiotactic polystyrene has been evaluated as an injection-molding resin due to its high melting temperature and high modulus [18]. In this molecule the phenyl ring attached to every other carbon is alternately above and below the plane of symmetry. In general, the production of three different stereo structures from the same monomer is performed using different polymerization catalysts. Polyethylene does not have stereoisomers because the two hydrogen atoms attached to a single carbon atom in the backbone are indistinguishable.

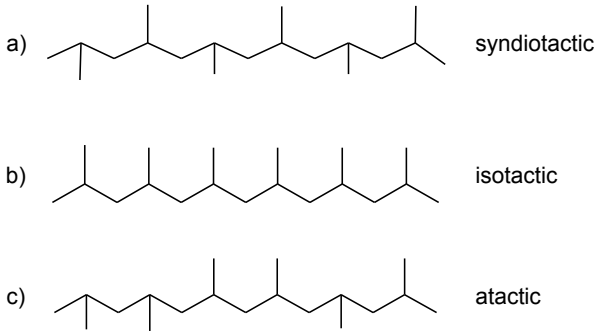

Figure 2.10 Structures of PP: a) syndiotactic, b) isotactic, and c) atactic

Stereoisomers are important in polymer production when carbon-carbon double bonds occur in the structure, as shown in Figure 2.11. This figure shows the classic chemical structure of the cis and trans isomers so well known in conventional chemistry and applied to polymers. They are sometimes known as the "boat" (cis) and "chair" (trans) configuration of molecular structure around the double bond. The location of these double bonds and the bulky units of the side chains can affect the average rotation time of the backbone bonds in these materials. As an example, butadiene can polymerize into a 1,2 or 1,4 configuration, and the structures will have very different chemical and physical properties. For the 1,4 polymerization product, the cis configuration has a melting temperature of 12 °C and the trans configuration at 142 °C. The cis and trans configurations of polyisoprene have different thermal properties. The cis configuration has a melting temperature of 28 °C while the trans configuration has a melting temperature of 80 °C. The trans configuration is used in many rubber compounds because its melting temperature is well above room temperature, and it is similar to natural rubber.

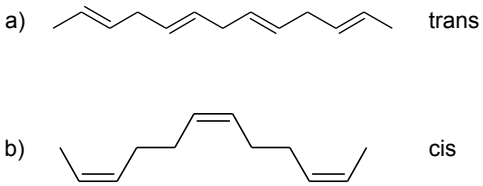

Figure 2.11 Double bonds in some rubbers: a) trans configuration, and b) cis configuration

2.3.2 Melting and Glass Transition Temperatures

The extruder temperature profile for a single-screw extruder is set such that the functions of the process convert the polymer from a "solid" to a "fluid." These two words are in quotation marks because for noncrystalline glassy (or amorphous) polymers there is no melting temperature. The melting temperature is defined as the peak temperature where most of the crystals are melted, and it will be dis-

cussed further in the next section. Since amorphous polymers do not contain crystal structures, they do not have a melting temperature. Amorphous polymers, however, undergo a change in properties at the glass transition temperature (T_g), and they are discharged from the extruder at a temperature substantially higher than the T_g. PS, PMMA, and PC resins appear as solids at room temperature because at room temperature the backbone carbon-carbon bonds rotate very slowly, and thus they only respond very slowly to an external stress. When they are below the T_g they act like a glass and not a fluid. As introduced earlier, the T_g is controlled by molecular motion as it relates to the backbone covalent bond frequency of rotation. In order for a carbon-carbon bond to rotate, the carbon that is rotating must overcome a potential energy barrier related to changing its relative position to the adjacent carbons. This energy barrier is due to the tetrahedral structure of the carbon covalent bonds. All of the structural changes discussed above in the molecular architecture (side chains and pendant groups), stereo structure, and double bond placement have a strong influence on the magnitude of this potential energy barrier and thus on the polymer's properties as a function of the environmental temperature and its glass transition temperature. The process for heating an amorphous resin from a temperature below the T_g to a temperature where the material is higher than the T_g is called devitrification.

At higher temperatures, the carbon-carbon backbone bonds will rotate at a higher frequency because there is sufficient molecular energy to counter the energy barrier that wants to keep the bond in a stable position. Thus, at higher relative temperatures the number of carbon-carbon backbone bond rotations per second increases. The increase in the rate of bond rotations is very small below the T_g due to the average bond potential energy being lower than the energy necessary for rotation. It is thus thought that the bonds only rotate essentially one at a time below T_g. When the bonds rotate many times per second, the polymer will be above its T_g, and it is usually thought that multiple groups of bonds have the energy to rotate simultaneously. The effect of side chains in general is to increase the potential energy barrier and thus require more thermal energy to increase bond rotation. It therefore follows that higher temperatures are required to get an equal rotation rate and multiple bonds rotating if molecules have large side chains. Natural rubber, poly 1,4 isoprene, has much smaller side chains than polystyrene. The trans stereo polymer of isoprene has a T_g of –50 °C. Natural rubber has many rotations at 25 °C but only a few rotations at –100 °C. At 25 °C it is well above its T_g, and it would flow under a slight force, or if slightly crosslinked it will stretch like a rubber band. At –100 °C it is below the T_g, and it would break like window glass if struck with a hammer. These differing responses to applied stresses relates to the ability of the molecule to dissipate energy and its ability to rotate the bonds in the backbone. In contrast, PS has many rotations at 150 °C and only a few rotations at 25 °C. The glass transition temperature for PS resin is about 100 °C. The difference

in rotation rates at comparable temperatures controls many of the properties and characteristics of polymers. For extrusion troubleshooting, the T_g sets the lower temperature limit for extruder operation since we need fluid-like behavior in the metering end of the extruder. Most amorphous resins will not flow well, however, until the temperature is 50 °C or more above the T_g. An excellent discussion on T_g with much more detail can be found elsewhere [1].

Polymers can thus be defined in general terms as "glassy polymers" for those resins with a T_g that is above room or use temperature, and as semicrystalline polymers that have a T_g well below room temperature and get their solid-like properties at use temperature because they have a crystalline phase. Semicrystalline polymers have a portion of the material that is completely amorphous, and thus this portion has a T_g. The polymer industry has over the years worked to develop the "ultimate" engineering polymer, which usually is partially crystalline. Like all fields of engineering there are exceptions to this, and PC is one of several exceptions. PC has a relatively high T_g of about 155 °C and has good impact strength in the glassy state at or near room temperature, unlike most glassy polymers such as PS or PMMA that fracture easily when impacted. An engineering polymer must have a very broad temperature use range. This can loosely be defined as the difference in temperature between the melting temperature (T_m) and the T_g. Over this temperature range partially crystalline polymers can be thought of as a flexible matrix of material above the T_g, held together by the high-modulus crystallites of the polymer acting as high-modulus fillers and physical crosslinks. Extensive early investigation of homogeneous polymers led to a relationship between T_g and T_m. Using absolute temperature the relationship was found that T_m is about 1.4 to 2.7 times the T_g of all homogenous polymers. For most polymers the melting temperature is thus a bounded function of the T_g. So the use temperature range is more or less constant for homogenous polymers. Although not discussed here, random and block copolymers do not follow this relationship.

2.3.3 Crystallinity

As discussed above, many polymers contain some crystalline structures when they are solidified. These polymers are referred to as semicrystalline resins. These crystalline structures can be observed using microscopy as shown in Figure 2.12 for PP and sPS resins. As shown schematically in Figure 2.13 and discussed above, not all portions of the polymer chains are incorporated into the crystalline structure. Instead, the portions of the chains that are not crystallized make up the amorphous phase. Solid density is the most commonly used method for measuring the degree of crystallinity in a polymer, especially for olefinic resins. LLDPE resins are common semicrystalline polymers, and have solid densities ranging from about

0.915 to 0.935 g/cm^3. Resins with higher solid densities contain higher levels of crystallinity and lower levels of the amorphous phase. For LLDPE resins, the crystallinity level is in general controlled by the amount of comonomer, that is, the amount of alpha olefin reacted into the polymer chain to create pendant groups. All PE resins are classified by their density: HDPE with a solid density greater than 0.940 g/cm^3, MDPE with a density range of 0.925 to 0.940 g/cm^3, LDPE with a range of 0.915 to 0.925 g/cm^3, and ULDPE with a density less than 0.915 g/cm^3.

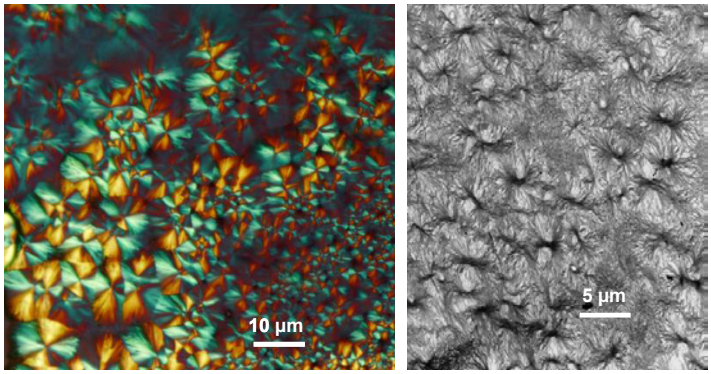

Figure 2.12 Photographs of polymer crystalline structures: a) optical photograph of PP resin using polarizing light and filters, and b) electron micrograph of sPS resin (courtesy of Robert C. Cieslinski of The Dow Chemical Company)

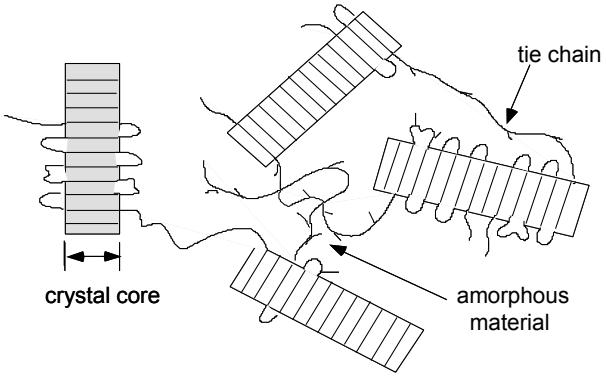

Figure 2.13 Schematic of the crystalline and amorphous regions of a semicrystalline polymer

Amorphous material often produces tie chains that connect two or more different crystals. These tie chains increase the properties of the solid resin by forming a temporary three-dimensional crosslinked system. As the resin is melted in an extruder, the crystals and the tie chains are destroyed, and the polymer acts like a normal thermoplastic resin. When the resin is cooled and solidified, the crystals and tie chains reform.

The level of short-chain (SCB) and long-chain (LCB) branches control the solid resin density of a PE resin. For example, the level of SCB is controlled by the amount of alpha olefin comonomer incorporated into LLDPE resin as a pendant group. The random positioning of the pendant groups disrupts the crystallization process when the polymer is cooled from the molten state, causing the level of crystallinity to decrease with increasing amounts of alpha olefin comonomer.

When semicrystalline polymers are heated in a differential scanning calorimeter (DSC), the temperature where the highest energy required for crystals to melt is referred to as the melting temperature (T_m). Figure 2.14 shows DSC heat flow curves for an LLDPE resin with a solid density of 0.935 g/cm^3 and a PP resin. The melting temperature of the PP resin (158 °C) is higher than that for the LLDPE resin (126 °C). As the polymer melts, a heat of fusion (area under the DSC curve during phase change) is determined, and the weight percent crystallinity can be calculated (100% crystallinity has a heat of fusion of 292 J/g for PE). Thus, a PE resin with heat of fusion of 100 J/g will contain about 34% crystalline material and 66% of the amorphous phase.

The modulus of PE resins increases with increasing solid density. Thus, a HDPE resin has a higher modulus than an LDPE resin, as shown by the data in Table 2.3. In general, resins with low solid densities feel "soft" to the touch while resins with high densities feel hard. The T_m and T_g for selected semicrystalline and amorphous materials are given in Table 2.3.

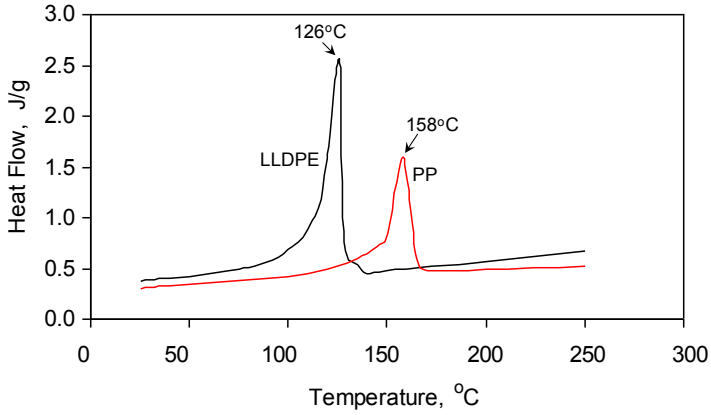

Figure 2.14 DSC heat flows for LLDPE and PP resins

Table 2.3 Physical Properties and Applications for Selected Resins

Resin	Tensile Modulus, MPa	Impact Strength, J/cm	Melting Temperature (T_m), °C (semicrystalline)	Glass Transition Temperature (T_g), °C (amorphous)	Applications
HDPE	1070 – 1090	0.2 – 2.1	135	(–110) to (–125)	Liners, sacks
HIPS	1100 – 2500	0.5 – 3.7		100	Packaging, specialty films
LDPE	170 – 280	No break	110	(–110) to (–125)	Films
LLDPE	260 – 520	No break	120	(–110) to (–125)	Films
PA 66	1600 – 3400	0.5 – 1.1	260	55 to 58	Barrier films
PET	2800 – 4100	0.13 – 0.37	240	78 to 80	Packaging films
PLA	3300 – 3800	0.03	160	55 to 60	Packaging, fibers
PP	1140 – 1550	0.2 – 0.75	170	–20 to –10	Packaging (sheet)
PS	3100 – 3300	0.20 – 0.24		100	Packaging, foam sheet
PVDC	340 – 550	0.1 – 0.5	165	–15	Oxygen and water barrier applications (food packaging)

The values given here are for resins with relatively low levels of additives. Resins with fillers or low molecular weight processing aids can have physical properties considerably different from these.

■ 2.4 Polymer Production and Reaction Engineering

This section introduces simple polymer reaction chemistry used to produce many commodity polymers. Understanding this simplified approach to the chemistry of polymer production is important in troubleshooting many extrusion processes, especially those that are producing unwanted degradation products that contaminate the discharge resin. There are two general types of polymer production processes: 1) step or condensation reactions, and 2) addition or vinyl polymerization reactions. An overview of the reaction mechanisms will be presented in the next sections.

2.4.1 Condensation Reactions

The classification of a condensation polymer is historically based on the observation that during polymerization a small molecule, such as water, is condensed or removed as part of the reaction. There are a large number of polymers produced from condensation reactions and only a representative sample is presented in Figure 2.15. Reactors for producing these materials include batch, continuously

vented, tray reactors, twin-screw extruders, and vented single-screw extruders. These production devices will not be covered in this text because they are of more interest to the manufacturing engineer than the extrusion process engineer.

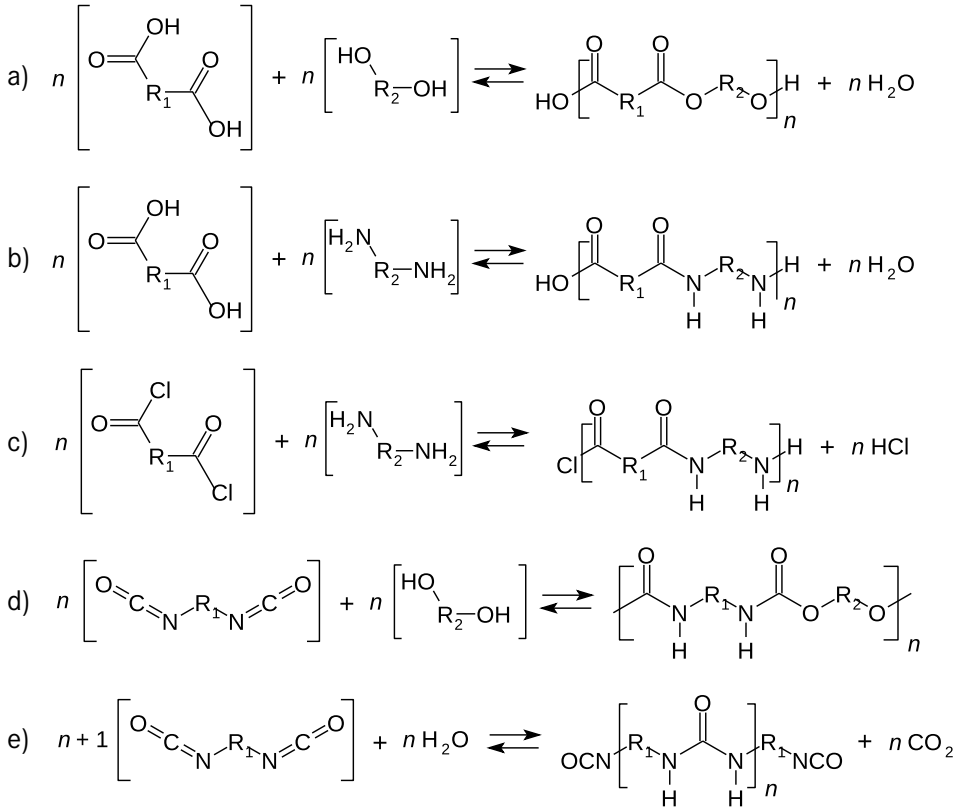

Figure 2.15 Reactions to produce typical condensation polymers: a) polyester, b) polyamide with water as a byproduct, c) polyamide with HCl as a byproduct, d) polyurethane, and e) polyurea

Not all of these polymers have a small molecule released during production, but they essentially all will react with water to reduce the polymer molecular weight during the extrusion process. Examining more closely the reactions in Figure 2.15, reaction (a) produces a polyester if the acid and base have two or more reactive acid and hydroxyl groups per molecule. If the number of reactive groups on each molecule is exactly two as shown then the product will be a linear polymer such as PET. If the average functionality is greater than two then an alkyd resin can be produced. In all of these reactions R_1 or R_2 represent the remainder of atoms that are attached to the reactive groups of the monomers. Reactions (b) and (c) produce polyamides. If R_1 and R_2 in reaction (b) are six-carbon linear chains and the monomer has reactive groups on both ends then the product will be PA 66. Reactions (d) and (e) are important in producing polyurethane thermoplastics and polyurethane foams. Reaction (d) produces a polyurethane by reaction of an isocyanate and an

organic alcohol. If the reactants are multifunctional a polymer is produced. A functionality of two produces a linear polymer while more than two produces a crosslinked polymer. Reaction (e) produces a polyurea, which is the product of an isocyanate and water. The evolved CO_2 is the blowing agent used to produce polyurethane foams, both rigid and flexible.

All chemical linkages in a condensation polymer have the potential to react at all times. For example, an acid end group on a chain that is *n* units in length can react with an alcohol end group on a chain that is *m* units in length, creating a new polyester chain that is $n + m$ units in length. Moreover, since the ester reactions are highly reversible, the new chain can hydrolyze into two smaller chains with lengths different than *n* and *m*. Because all the bonds can react at any time, these reactions are characterized by Gaussian statistics, and thus the molecules grow or decompose as a result of random event polymerization or hydrolysis of the reactive groups, respectively. Thus, the final resin will have a distribution of chains with different molecular weights; the weight average will approach two times the number average molecular weight. The length and distribution will affect its end-use physical and rheological properties. High molecular weight polymers only come at very high conversion of the monomer to polymer, which is when the small condensation molecules have been removed from the reaction mixture. All of the process reactors for the polymers listed above are thus vented and usually attached to strong vacuum systems. Also, the production of high molecular weight polymers (high average *n* values) only occurs when the reactive groups are present at equimolar concentrations. That is, there is the same number of the two reactant species in the reactor at the beginning of the polymerization. Only when many of the molecules in the reacting mass are connected as a polymer molecule and when essentially all of the monomer has been reacted into the polymer is a high molecular weight polymer produced with good physical properties.

In addition to condensation reactions, ring-opening reactions are often used to produce polyethers and polyamides. The most well known polyether and polyamide are polyethylene glycol and PA 6, as shown in Figure 2.16. Both are considered condensation polymers and are produced from cyclic monomers. Polyethers are somewhat more stable to hydrolysis than most other condensation polymers, but they are, however, degraded by reaction with adsorbed water, and they thermodynamically rapidly decompose at temperatures above 500 °C. Reaction (a) in Figure 2.16 produces polyethylene glycol. Ring opening in Figure 2.16(b) is also used to produce PA 6 from caprolactam. Polytetrahydrofuran is produced from the ring opening of tetrahydrofuran, and it is a semicrystalline polyol used in many high-modulus polyurethanes. The mechanism for these reactions is quite complex and the reader should consult a text on polymer chemistry or polymer materials [1, 19] for a thorough discussion of ring-opening reactions. It is important to emphasize again that all of these polymers can be susceptible to degradation due to the

attack of water molecules in the extruded polymer, leading to hydrolysis and the loss of physical properties in the finished product.

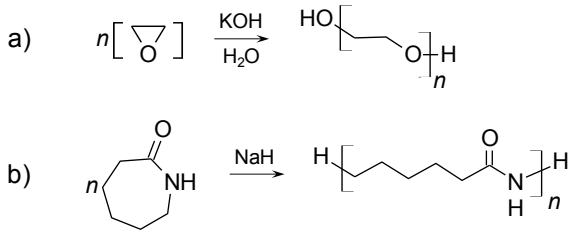

Figure 2.16 Ring-opening catalyzed condensation polymers: a) reaction for polyethylene oxide, and b) caprolactam ring opening to PA 6

2.4.2 Addition Reactions

Addition reactions are used to produce vinyl polymers, and several commercial monomers are presented in Figure 2.17 In this route to a high molecular weight polymer, the monomer has at least one double bond and often a larger number of nonreactive functional or pendant groups. This type of polymerization is often called addition or chain polymerization. During the reaction of a bulk polymerization of vinyl monomers, only certain activated species react, only a few chains grow at once, and a high molecular weight polymer is obtained quickly. Addition reactions are controlled by active centers. This mechanism is entirely opposite to the reaction mechanism for condensation polymers. As discussed previously, condensation reactions occur with many chains growing and decomposing at once, and high molecular weights depend on equimolar amounts of the two reactants.

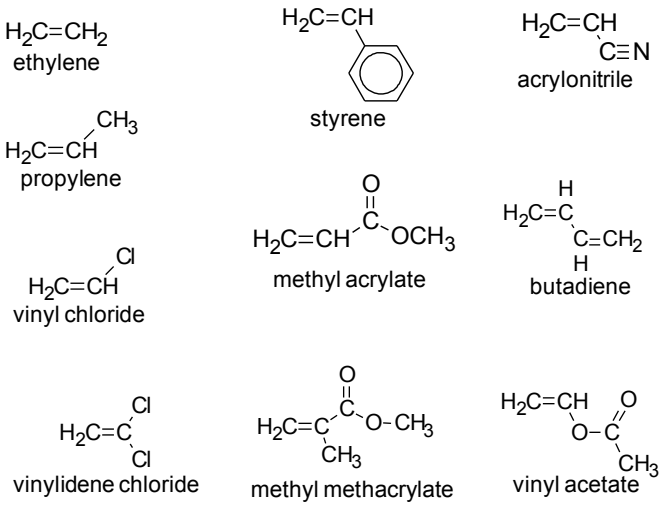

Figure 2.17 Typical vinyl monomers

The active centers can typically be free radicals, positive ions, negative ions, or a metallic catalyst. The metallic catalysts include Ziegler-Natta catalysts and chromium derivatives, and metallocene catalysts. Metallocene catalysts are typically cyclopentadienyl derivatives of a transition metal. Most of these polymers are traditionally made in bulk from vinyl monomer and free radicals. Many are polymerized in solvents with either homogenous or heterogeneous catalysts. Some polymers such as those produced by the low-pressure gas phase process use Ziegler-Natta catalysts that have the catalyst supported on a solid substrate. However, more and more of these vinyl polymers are now being produced using metallocene catalysts because this technology, which became commercially economical in the 1990s, leads to better control of the polymer molecular structure and thus the physical properties.

The use of free radicals, positive ions, or negative ions for the polymerization depends on the monomer and the pendant group. Monomers with strong electron-withdrawing groups can be polymerized with anions to form stable carbanions. Strong electron-donating groups on the vinyl monomer lead to polymerization with cations to form stable carboniums. Vinyl monomers with intermediate electron characteristics (not strongly withdrawing or strongly donating) polymerize with free radicals produced by molecules that decompose, leaving an unpaired electron, as shown in Figure 2.18. Some monomers such as ethylene, styrene, and butadiene will polymerize by essentially any of the above methods. Four typical free radical initiators are benzoyl peroxide, AIBN, and t-butyl-hydroperoxide, and potassium persulfate, as shown in Figure 2.18. Potassium persulfate is one of the few materials that will produce stable free radicals in water, and thus it is used extensively in emulsion polymerization. Due to the mechanism of growth of the polymer inside a soap micelle in emulsion polymerization, very high molecular weight polymers are produced because it is difficult for a second free radical to enter the micelle. The fragments of the free radical initiator molecule can thus terminate the resulting polymer molecule when the growing polymer chain encounters a free radical, as is the case almost exclusively in emulsion polymerization. In each of these cases, the free radical is indicated by (•), as shown in Figure 2.18.

The reaction sequence for a typical vinyl polymer has four steps. In the first step, a free radical must be produced from the initiator such as those shown in Figure 2.18 and Figure 2.19. These radical formation reactions are typically first order in rate and are promoted by the elevated temperature of the reaction. For some free radical initiators, light can also promote the reaction. Then a sequence of events in the reaction mixture occurs, including initiation of a chain, followed by propagation, and finally termination of the chain. Termination of the chain will be discussed later. The schematic steps to produce an addition polymer from bulk or solvent polymerization are detailed in Figure 2.19. The radical produced from the

initiator reacts with the monomer in Step 2 to produce a new free radical by opening the double bond of a vinyl monomer. The active center of the new radical is at the opposite end of the activated mer. Propagation (Step 3) occurs when the active center reacts with more monomer and continues to add more monomer, one mer at a time. This propagation step continues until a termination reaction ends the process.

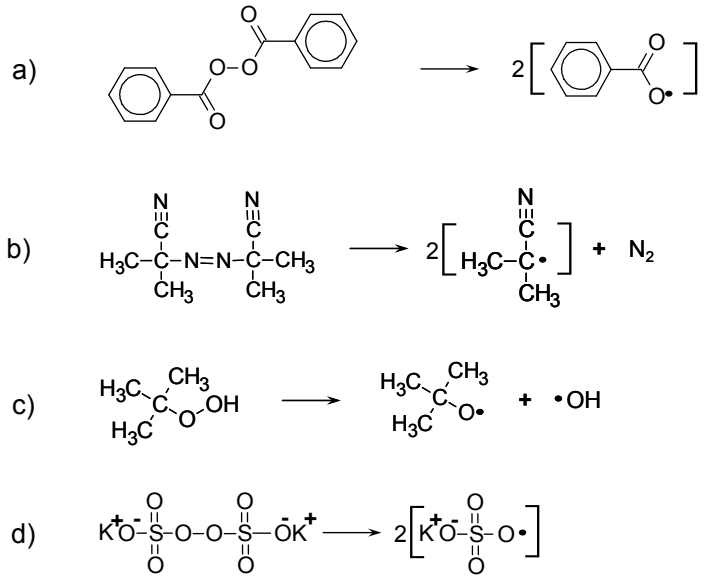

Figure 2.18 Four free radical initiators: a) benzoyl peroxide, b) azobisisobutylnitrile (AIBN), c) t-butylhydroperoxide, and d) potassium persulfate; (•) is the free radical

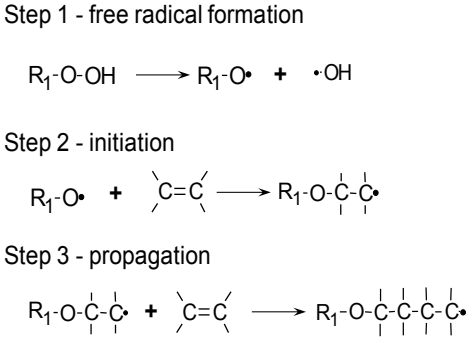

Figure 2.19 Addition polymer free radical formation, initiation of the monomer, and propagation

Termination (Step 4) can normally occur by either combination or disproportionation reactions, as shown in Figure 2.20. For a combination termination, two chains with active centers combine to form a new chain without an active center. The molecular weight of the chain produced is the sum of both radicals. If these are two relatively large growing chains, a very high molecular weight polymer is obtained.

If large and small chains are combined, then a much smaller molecule is produced. If one of these radicals is a growing polymer and the other a free radical derivative of the decomposition of the initiator, a molecule that is about the size of the propagating molecule terminated on both ends by initiator fragments is formed. For the disproportionation termination, a hydrogen atom with its electron is extracted from one of the radicals, creating a polymer chain that is saturated and a polymer chain with a double bond at the very end of the chain, as shown in Figure 2.20. These different termination mechanisms cause the bulk polymerized materials to have very broad molecular weight distributions. Polymerizations that produce terminal double bonds can cause problems during extrusion. The double bonds can react with oxygen to create a new free radical. The free radical can then continue to react, forming links, branching, and degradation products [12] in the extruder.

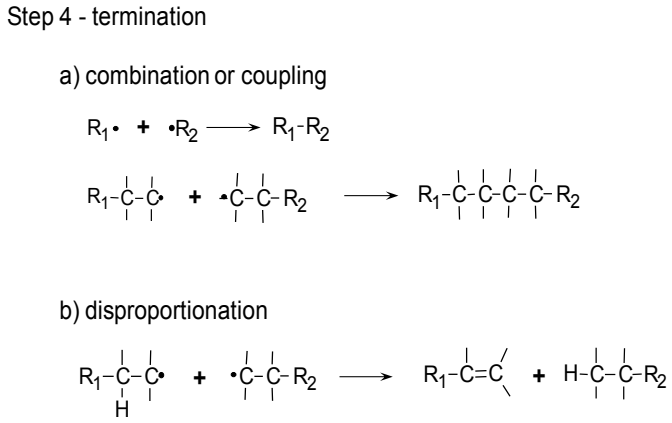

Figure 2.20 Termination of addition reactions

Many polymers are produced using addition reactions, including PE resins, PP, PS, to name just a few. Moreover, there are many different reactor styles and comonomers used to produce PE resins. These methods and the resin stuctures that they produce are beyond the scope of this work, but they can be obtained in reference [20].

■ 2.5 Polymer Degradation

The polymer industry works very diligently to produce high-quality polymers. All of these polymeric materials, however, are subject to substantial degradation under the conditions found in most extruders unless precautions are taken to minimize the reactions. The degradation can be broadly classified into three areas. Degrada-

tion of addition polymers is associated with the loss of a hydrogen atom, usually due to high shear stress related to high polymer viscosity. The resulting radical reacts with oxygen from the atmosphere to form a peroxide, reacting with a double bond to form a branch and eventually a crosslinked gel. For condensation polymers the major form of degradation is attack by absorbed water that comes from the humidity in the air, causing a loss in molecular weight. Condensation resins can also undergo attack from free radicals, resulting in black colored char. Finally for chlorine- and fluorine-containing compounds such as PVC, PVDC, and PVDF, a major mechanism for degradation is the formation of HCl or HF and the subsequent crosslinking of the polymer into a black char. These reactions once initiated are very rapid and can be catalyzed by brass or other metals.

In order to minimize the degradation of a polymer when it is extruded, resin manufacturers add stabilization chemicals to the resin. Often the term resin is used for a polymer that contains additives. Moreover, ultraviolet stabilizers are often added to minimize the attack from light on the extruded and injection-molded parts. For example, resin manufacturers add oxidation stabilization packages to nearly all addition polymers to minimize degradation in normal extrusion operations. These compounds are free radical scavengers. These compounds, however, are "consumed" in the extruder over time because they are destroyed as they react with oxygen and free radicals in the polymer melt. Thus, these radicals have a minimum effect on the polymer as long as there is antioxidant still available in the polymer melt. Once these oxidation stabilizers are consumed by multiple passes of the polymer through the extruder, the polymer will potentially degrade in the extruder. Multiple passes typically occur with processes that utilize a very high regrind rate. Moreover, if the extrusion process is improperly designed such that stagnation regions exist, then the resin will be exposed to high temperatures for a very long time, creating the formation of degradation products. Another issue is "old" polymer that has been stored in a warehouse for extended periods of time. In this case, the antioxidants will slowly lose effectiveness. Commonly used antioxidants and their mechanism for protecting PE resins from degradation can be found in [21].

Improperly designed processes can be highly prone to discharging degradation products into the final product. If the process involves hydrolysis such as occurs with the inclusion of water for a condensation polymer, the resin in the final product will have a considerably lower molecular weight and thus deminished physical properties. In these cases, the final product may need to be discarded because the physical properties do not meet the product specification. If a region exists in the process where the flow is stagnant, then the resin in the region can have essentially an infinite residence time, allowing the resin to degrade via oxidation. The degradation products typically stay in the stagnant region until a minor process disruption occurs. The disruption will cause some of the degraded resin to move

from the stagnant region into the main flow path. The degradation products will then flow downstream and contaminate the final product. The physical forms of the degradation products for several common polymers are shown in Table 2.4. Troubleshooting processes that have degradation products occurring in the final product are discussed in Chapter 11.

Table 2.4 Degradation Products for Common Polymers

Resin	Physical Products Formed
ABS, HIPS	Styrene monomer, black specks
Acetal	Loss of molecular weight – acid hydrolysis and oxidation
PA	Loss of molecular weight by hydrolysis with water contamination
PBT	Loss of molecular weight by hydrolysis with water contamination
PC	Loss of molecular weight by hydrolysis with water contamination, black specks
PE	Crosslinked resin (gels)
PEN	Loss of molecular weight by hydrolysis with water contamination
PEEK	Breaking of ether bonds, reducing molecular weight
PET	Loss of molecular weight by hydrolysis with water contamination
PMMA	Methyl methacrylate monomer, black specks
PP	Loss of molecular weight via chain scission
PPO/HIPS blend	Black specks from oxidation and styrene monomer
PS	Styrene monomer, brown-colored resin
PVC, PVDC	HCl generation by dehydrochlorination, black specks
PVDF	HF generation by dehydrofluorination, black specks
SAN	Styrene monomer, black specks
SBS	Crosslinked gels
SIS	Loss of molecular weight by chain scission
sPS	Styrene monomer
TPU	Loss of molecular weight with water contamination, resin can turn yellow

As shown in Table 2.4, PE resins will crosslink during the degradation process. Since the molecular architecture is very broad for this class of materials, the degradation process and rates are also broad. For example, LDPE resins produced from the high-pressure process are the most stable to oxidation. In Section 11.10.1 an improperly designed process operated without discharging degradation products for about 13 days, but after 13 days the process was discharging crosslinked gels to the product. Thus, the resin required about 13 days of residence time in this case to degrade the resin to a detectable defect. LLDPE resins are considerably less stable. The formation of gels at processing temperatures can occur in as little as 20 minutes in stagnated regions.

The next sections will present an overview of the relative susceptibility of different polymers to degradation reactions. For a more in-depth discussion the reader is encouraged to consult the open literature for the resin. Mitigating these types of degradation reactions is highly important in order to maintain the ultimate physical properties of the final product and eliminate degradation products in the extrudate. Several case studies relating to resin degradation and contamination will be presented in Chapter 11.

2.5.1 Ceiling Temperature

The heat of reaction for vinyl polymers affects the thermal stability of the polymer during extrusion, and the thermal stability is related to the ceiling temperature. The ceiling temperature is the temperature where the polymerization reaction equilibrium is shifted so that the monomer will not polymerize, or if kept at this temperature all the polymer will be converted back to monomer. From thermodynamics the equilibrium constant for any reaction is a function of the heat of reaction and the entropy of the reaction. For PS resin, the exothermic heat of reaction for polymerization is 70 kJ/gmol, and the ceiling temperature is 310 °C. Ceiling temperatures for select polymers are shown in Table 2.5.

Table 2.5 Ceiling Temperatures and Heats of Reaction (Exothermic) for Select Polymers

	Heat of Reaction, kJ/gmol	Ceiling Temperature, °C
Poly(α methyl styrene)	33	61
PMMA	54	220
PS	70	310
PE	94	400
PVC	109	–

Thus there is an equilibrium concentration between monomer and polymer at high temperatures such that both the monomer and polymer are present. In order to mitigate the formation of monomer, the extruder must be operated at temperatures considerably less than the ceiling temperature. The ceiling temperature is determined from the equilibrium thermodynamics of the reaction. For polymerization reactions that have negative enthalpy of polymerization, the temperature above which a monomer cannot be converted to a long-chain polymer is controlled by the Gibbs free energy ΔG:

$$\Delta G = 0 = \Delta H - T\Delta S \tag{2.1}$$

where ΔH is the heat of polymerization and ΔS is the entropy change. At equilibrium by a thermodynamic definition, the Gibbs free energy change ΔG is equal to 0. This leads to a simple calculation for the ceiling temperature where equilibrium is achieved:

$$T_c = \frac{\Delta H}{\Delta S} \tag{2.2}$$

where T_c is defined as the ceiling temperature for the polymerization in degrees Kelvin. Further details on the thermodynamic concept of free energy can be obtained in any thermodynamics text. The processing importance here is that the polymer will produce monomer in the extruder as the ceiling temperature is approached. In other words the polymer will rapidly depolymerize due to a thermodynamic driving force, and no stabilizer can prevent the reaction. From the data in Table 2.5 and Equation 2.2, the ceiling temperature is directly proportional to the heat of polymerization. All vinyl polymerizations have exothermic heats of reaction. If the heat of the polymerization reaction is known, then the ceiling temperature can be estimated for other polymers from the data in Table 2.5. The more heat that is evolved during the reaction to produce the polymer the higher the ceiling temperature and thus thermodynamic stability of the polymer. This equilibrium shift, however, does not suddenly occur at the ceiling temperature. Instead, the evolution of monomer will start to occur at temperatures considerably less than the ceiling temperature. For example, during the extrusion of PS resin at 200 °C, a small amount of styrene monomer can be detected via smell at the die, a temperature that is about 110 °C less than the ceiling temperature. For PMMA, methyl methacrylate monomer is detected at all reasonable extrusion temperatures. Both PS and PMMA resins degrade by the evolution of a monomer unit one at a time from the end of the chains. This is why the property loss is slower for these resins than that for the hydrolysis of condensation polymers where the chains are randomly broken. For many vinyl polymers the loss of monomer is more random in chain location and the properties will be lost more rapidly than in the case of PS resin. This is an important degradation mechanism for polymers and very often not understood by the extrusion engineer or operator as the cause of production problems. If recycled resin is passed through an extruder multiple times, the degradation reactions can quickly diminish the physical properties to an unacceptable level.

The exothermic heat of reaction for PVC is relatively high, and thus so is the ceiling temperature. PVC resins, however, will dehydrohalogenate at temperatures considerably lower than the ceiling temperature, forming HCl gas and charred material. In this case, thermal degradation reactions occur at temperatures less than the ceiling temperature.

The ceiling temperature for sPS resin is the same as that for atactic PS (or just PS). Due to the crystalline structure of sPS resin, the melting temperature is about 270 °C and the processing temperature is about 290 °C. At these temperatures and with a ceiling temperature of 310 °C, a considerable level of depolymerization and evolution of styrene monomer occurs during processing. Although the high melting temperature of sPS provides a material that has a high resistance to heat and chemicals, the processing window is very narrow since the melting temperature is only 40 °C lower than the ceiling temperature. Due to this small temperature processing window, it is important to minimize the time that the polymer experiences the high temperatures of the processing step.

2.5.2 Degradation of Vinyl Polymers

Oxygen radicals are well known for their attack on hydrogen atoms at the conditions existing in an extruder. These attacks are different for hydrogen atoms that are in different configurations in the polymer molecule. For example, the relative stability and thus ease of formation of a radical is higher for the abstraction of hydrogens attached to tertiary carbons of a PP resin as compared to hydrogens attached to secondary and primary carbons, as shown by Figure 2.21. Thus, the easiest mode of oxygen radical attack on a PP molecule will preferentially occur at the hydrogens attached to tertiary carbons. Preferential oxygen radical attacks on hydrogens of polypropylene glycol and trans polyisoprene are shown in Figure 2.21. Moreover, the relative rates of attack by oxygen radicals on the hydrogen atoms, shown by the arrows in Figure 2.21, are reported to be 6.5 for PP, 9 for polypropylene glycol, and 10 for trans polyisoprene [2]. The attack on the backbone hydrogen in PE resins by oxygen radicals is quite low unless there are residual double bonds (unsaturation), very long thermal residence times, or very high shear stresses such as found in the gap between the screw flight and the barrel. HDPE resin produced using a chromium-type catalyst in the Phillips process is reported to have a double bond in each molecule, so it is susceptible to attack by free radicals [15]. When metallocene-catalyzed polymers were introduced for the production of PE films, it was found that antioxidants were very important in producing stable products for extrusion processes.

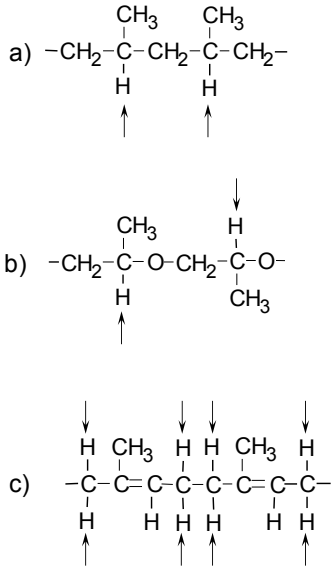

Figure 2.21 Most probable hydrogens attacked by oxidation: a) PP resin segment, b) polypropylene glycol segment, and c) trans polyisoprene segment. The arrows point to the hydrogens that are the most susceptible to attack and removal

In general the oxidation process for polymers in an extruder occurs in a sequential process similar to the process for producing the polymer. The oxidative degradation process for vinyl polymers is shown in Figure 2.22. For this process, a radical must be produced first. The hydrogen atoms shown in Figure 2.21 can be abstracted by high local shear stress such as found in the barrel-flight gap in the extruder, producing a process symbolized as a free radical in Step 1. Also, oxygen can attack to form a radical at high enough temperatures. The radicals can then propagate as shown in Step 2. High temperatures accelerate these attacks on the polymer structure. Moreover, high temperatures coupled with regions in the process with very long residence times will almost always lead to degradation products. These regions are often found in improperly designed flight radii, partially filled metering channels, and mixing sections. As discussed previously, oxygen is not a chain former, and thus two adjacent oxygen atoms in the polymer backbone will be unstable such as in Step 2. In Step 2 one of the propagation products is a peroxide, which can decompose on heating to form a new radical and further attack the polymer. The reaction in Step 3 can lead to crosslinks that appear as gels or to char-like materials that eventually appear as black specks in the finished product. The peroxide in Step 3 can also decompose on heating to produce more radicals. As stated previously, the resin manufacturers typically add antioxidants to the resins after they are produced so that oxidation is minimized in the extruder during processing. These stabilization packages can contain phenolic stabilizers, organophosphorus compounds, lactones, and hydroxylamine compounds as well as other materials.

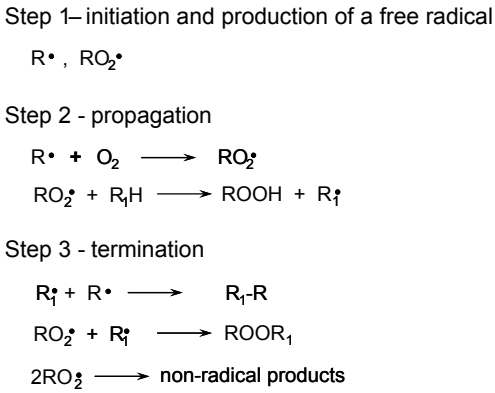

Figure 2.22 Oxidation mechanism for vinyl polymers

As introduced previously, the compounds in stabilizer packages are consumed with time and thus they will be eventually depleted. As expected, the consumption rate will depend on the temperature and residence times for the resin. Thus, it is important to minimize the number of recycles for a product stream and excessively high temperatures in the extruder. For example, LLDPE resin produced using a metallocene catalyst showed an increase in the molecular weight as measured by a decreasing flow index, yellowing of the sample, and consumption of stabilizers with multiple passes through an extruder [22, 23]. After the stabilizers are consumed, the rate of polymer oxidation to unwanted byproducts such as gels and black specks will accelerate. The type of degradation is dependent on the polymer structure. For example, PE and PP resins contain only carbon and hydrogen atoms, yet their degradation mechanism and products are drastically different. Free radical attack on PE resin almost always results in long-branched polymers and local crosslinks (gels in film production), and the continued degradation will produce a carbonaceous material usually described as black specks in the product. PP resins, however, will degrade in a very different manner via scission of the molecule by free radical attack, causing a substantial decrease in molecular weight and thus the physical properties. Chain scission using peroxides [24, 25] is a common manufacturing method of producing high melt flow PP resins from low melt flow reactor products.

2.5.3 Degradation of Condensation Polymers

As presented in Section 2.4.1, all condensation polymers will react with water, and these reactions are equilibrium reaction systems. Water is absorbed by all of these polymers due to the polar nature of the bonds that form the polymer. If the absorbed water is not removed prior to processing, the water can cause the polymer to hydro-

lyze at the high temperatures of processing, reducing the molecular weight. Equations (a) and (b) in Figure 2.15 are the reversible reactions used to form polyester and PA resins, respectively. These materials can absorb as much as 5% water when stored in high-humidity conditions in a warehouse. The hydrolysis reaction rate is very low at room temperature, so the highly absorbed water content does not in general hurt the polymer structure over normal storage times. But at the high temperatures in an extruder this reaction is quite fast, and the polymer will be destroyed unless it is dried before extrusion. It is reported that 5% water can be absorbed in PA 66 resin at nominal storage conditions [1]. This absorbed water would destroy about one-third of the amide bonds at equilibrium and reduce the polymer to a material having no usable physical properties. Polyesters, polyurethanes, polycarbonate, and polyacetals must also be dried prior to extrusion. Extruding any of these materials without proper drying will lead to a great loss in properties. Polycarbonate and polyacetal are somewhat more resistant to hydrolysis degradation than polyurethanes and polyesters. For PET it could be expected that the intrinsic viscosity (IV) of poorly dried polymer would easily decrease from about 0.9 dl/g to about 0.6 dl/g for one pass through the extruder. This decrease in IV indicates a substantial decrease in molecular weight and thus the physical properties of the final product.

References

1. Rodriguez, F., "Principles of Polymer Systems," 4th ed., Taylor & Francis, Washington, DC (1996)
2. Rodriguez, F., Cohen, C., Ober, C. K., and Arcer, L. A., "Principles of Polymer Systems," 5th ed., Taylor & Francis, Washington, DC (2003)
3. Walker, P., "Trends in Manufacturing Polymers: Achieving High Performance in a Multi-Polar World," Accenture (2009)
4. Paquet, A., Chum, S., and Rubens, L. C., "Extruded STYROFOAM™ and ETHAFOAM™ Products; Historical Perspective," *SPE ANTEC Tech. Papers*, **49**, 3801 (2003)
5. Avérous, L. and Halley, P. J., "Biocomposites Based on Plasticized Starch," *Biofuels, Bioprod. Biorefin.*, **3**, 329 (2009)
6. Xie, F., Yu, L., Liu, H., and Chen, L., "Starch Modification Using Reactive Extrusion," *Starch/Stärke*, **58**, 131 (2006)
7. Jacobsen, S., Degee, P. H., Fritz, H. G., Dubois, P. H., and Jerome, R., "Polylactide (PLA): A New Way of Production," *Polym. Eng. Sci.*, **39**, 1311 (1999)
8. Iliuta, M. C. and Larachi, F., "Solubility of Total Reduced Sulfurs (Hydrogen Sulfide, Methyl Mercaptan, Dimethyl Sulfide, and Dimethyl Disulfide) in Liquids," *J. Chem. Eng. Data*, **52**, 2 (2007)

9. Harris, P.J. and Smith, B.G., "Plant Cell Walls and Cell-Wall Polysaccharides: Structures, Properties and Uses in Food Products," *Int. J. Food Sci. Technol.*, **41**, 129 (2006)
10. Ito, H., Kumari, R., Takatani, M., Okamoto, T., Hattori, H., and Fujiyoshi, I., "Viscoelastic Evaluation of Effects of Fiber Size and Composition on Cellulose-Polypropylene Composite of High Filler Content," *Polym. Eng. Sci.*, **48**, 415 (2008)
11. Cieslinski, A., "An Introduction to Rubber Technology," Elsevier Science & Technology Books, St. Louis (2000)
12. Swogger, K.W., Carnahan, E.M., Hoenig, W.D., and Frencham, A.R., "The Development of a New Generation of Novel High Performance Olefin Elastomers: From Molecular Design to Market Development," *SPE ANTEC Tech. Papers*, **52**, 1008 (2006)
13. Swogger, K.W., "An Outlook for Metallocene and Single Site Catalyst Technology into the 21st Century," *SPE ANTEC Tech. Papers*, **44**, 1790 (1998)
14. Hiltner, A., Wang, H., Khariwala, D., Cheung, W., Chum, S., and Baer, E., "Solid State Structure and Properties of Novel High Performance Olefin Elastomers," *SPE ANTEC Tech. Papers*, **52**, 1000 (2006)
15. Epacher, E., Krohnke, C. and Pukhanszky, B., "Effect of Catalyst Residues on the Chain Structure and Properties of a Phillips Type Polyethylene," *Polym. Eng. Sci.*, **40**, 1458 (2000)
16. Wakeman, I.B. and Johnson, H.R., "Vinyl Chloride Formation from the Thermal Degradation of Poly(Vinyl Chloride)," *Polym. Eng. Sci.*, **18**, 404 (1978)
17. Hsieh, T-H. and Ho, K-S., "Thermal Dehydrochlorination of Poly(vinylidene chloride)," *J. Polym. Sci., Part A-1: Polym. Chem.*, **37**, 2035 (1999)
18. Schellenberg, J. and Leder, H-J., "Syndiotactic Polystyrene: Process and Applications," *Adv. Polym. Technol.*, **25**, 141 (2006)
19. Hiemenz, P.C. and Lodge, T.P., "Polymer Chemistry," 2nd ed., CRC Press, Taylor & Francis (2007)
20. Spalding, M.A. and Chatterjee, A.M., editors "Handbook of Industrial Polyethylene and Technology," Wiley – Scrivener Publishing, Hoboken, NJ, 2017.
21. Fay, J. and King, R.E. III, "Degradation and Stabilization of Polyethylene," Chapter 23 of "Handbook of Industrial Polyethylene and Technology," Spalding, M.A. and Chatterjee, A.M., editors, Wiley – Scrivener Publishing, Hoboken, NJ, 2017.
22. Hoang, E.M., Liauw, C.M., Allen, N.S., Fontan, E., and Lafuente, P., "Effect of Metal Stearate Antacid on the Melt Stabilization Performance of Phenolic/Phosphite Antioxidants in Metallocene LLDPE. Part 1: Melt Processing Stability," *J. Vinyl Addit. Technol.*, **10**, 3, 137 (2004)
23. Hoang, E.M., Liauw, C.M., Allen, N.S., Fontan, E., and Lafuente, P. "Effect of Metal Stearate Antacid on the Melt Stabilization Performance of Phenolic/Phosphite Antioxidants in Metallocene LLDPE. Part 2: Discoloration," *J. Vinyl Addit. Technol.*, **10**, 3, 144 (2004)
24. Tzoganakis, C., Vlachopoulos, J., and Hamielec, A.E., "Production of Controlled-Rheology Polypropylene Resins by Peroxide Promoted Degradation During Extrusion," *Polym. Eng. Sci.*, **28**, 170 (1988)

25. Scorah, M.J., Zhu, S., Psarreas, A., McManus, N.T., Dhib, R., Tzoganakis, C., and Penlidis, A., "Peroxide-Controlled Degradation of Polypropylene Using a Tetra-Functional Initiator," *Polym. Eng. Sci.*, **49**, 1760 (2009)

3 Introduction to Polymer Rheology for Extrusion

Polymers have numerous physical properties that are important to processing. The most important of these properties is their rheological response to flow. This chapter will introduce the basic concepts of rheology, the effect of molecular weight, molecular weight distribution, and structure on viscosity, and its measurement. As discussed in Chapter 1, the shear viscosity of a resin is highly important for calculating the pressure-driven flow in the channel in the metering section. Moreover, the shear viscosity also affects many other aspects of extrusion including the ability of the machine to generate pressure and dissipate energy, the discharge temperature, and the melting process. Process calculations, screw design, and troubleshooting all require viscosity data. Other physical properties related to processing will be presented in Chapter 4.

3.1 Introduction to the Deformation of Materials

When a material is extruded it is deformed, causing the material to change shape both macroscopically and microscopically. This deformation occurs in the extruder, in downstream processing equipment, and in the die. The study of the deformation of materials is called rheology. This chapter introduces several important aspects of polymer rheology that are required for extruder design and troubleshooting, that is, it provides an understanding of the relationship between the forces imposed on the polymer melt and the resulting deformation. The focus will be on engineering models for quantitative evaluation of the resistance to flow and deformation of polymer melts to applied forces. The chapter does not present the fundamental theories that relate polymer deformation to molecular structure. These details would be covered in a course or text on the fundamentals of rheology, and they are beyond the scope of this chapter.

The shear rate and shear stress associated with the resistance to flow of polymer melts in extruders are related to viscous energy dissipation, temperature changes, and the extrudate temperature. These interactions are important concepts used by the screw designer when seeking to evaluate the optimum operation of extruders and dies and in particular the pressure gradients and temperature changes due to the flow of the polymer in the screw channels and in the die cavity. In this chapter three aspects of polymer rheology will be discussed: Newtonian viscosity, shear-rate-dependent viscosity, and a very brief introduction to the concept of the dynamic viscoelastic properties of polymers. Viscoelasticity can have a strong effect on the mixing in some designs of single-screw processes, especially when the mixing section causes the polymer melt to be stretched or elongated.

Almost all aspects of polymer rheological properties are related to the polymer molecular weight, molecular weight distribution, and polymer molecular structure. A polymer's resistance to deformation is also a function of the chemical composition of the mer, the temperature, and the strain rate that is applied. In the previous chapter several important chemical-based properties of polymers were introduced and discussed. The concepts included molecular architecture, crystalline and amorphous structures, stereoisomers, pendant groups, branches, and crosslinks. In this chapter those basic polymer concepts are expanded to include polymer molecular weight and molecular weight distribution. Since the molecular weight of a polymer is a primary factor influencing many rheological characteristics of polymeric materials, a discussion of molecular weight is developed here as a background for relating polymer molecular structure to basic rheological responses of polymers.

3.2 Introduction to Basic Concepts of Molecular Size

The concepts of polymer molecular weight averages and molecular weight distribution will now be developed. Unlike small molecules like sodium chloride with a molecular weight of 58.45 kg/kg-mol and simple organic compounds like propane and ethanol with molecular weights of 44.09 and 46.07 kg/kg-mol, respectively, polymers essentially never have a single well-defined molecular weight. Instead the molecular weight of polymers must be discussed in terms of averages of distributions of molecular size. When working with polymers as they relate to extrusion there are several average molecular weights typically defined: number average molecular weight, M_n; weight average molecular weight, M_w; z average molecular weight, M_z; and the $z + 1$ average molecular weight, M_{z+1}. These different represen-

tations of polymer molecular weight, and thus average size, all have important bearings on how to characterize the properties of polymers. The relative size of these averages influences how the polymer responds to shear stress and shear rate. The use of some of these concepts is discussed more completely later in the chapter as they are the most important parameters related to the flow resistance of polymer melts.

3.2.1 Size Distribution Example

An example of size distribution is described here as an illustration of length, area, and volume distributions. A collection of particles, in this case large particles [1], will be analyzed regarding several distributions related to particle diameters. The following discussion regarding distributions is summarized in Table 3.1. How would you answer this question: would you be willing to catch 1000 steel balls with an average diameter of 6.1 cm [1]? Many would assume these balls are about the same size and say yes. It is important to understand that there are many types of averages that can be calculated. These particular particles are relatively large. They are a collection of 1000 steel balls. Nine hundred of the balls have a diameter of 2.54 cm. Fifty balls have a diameter of 12.7 cm and 50 have a diameter of 63.5 cm. A length dimension would be the number of balls of a particular size times the diameter. An area dimension would be the number of balls multiplied by the diameter squared, and a volume dimension would be the number of balls times the diameter cubed. These transformations are summarized in Table 3.1 along with the summations on the particular dimensional function. The length, area, and volume average diameters are calculated using Equation 3.1, Equation 3.2, and Equation 3.3, respectively.

Table 3.1 Summary of Distribution Explanation

Number of Balls N_i	Ball Diameter D_i, cm	Length N_iD_i, cm	Area $N_iD_i^2$, cm^2	Volume $N_iD_i^3$, cm^3
900	2.54	2286	5806	14,750
50	12.7	635	8065	102,420
50	63.5	3175	201,613	12,802,000
	Sum of column:	6096	215,484	12,919,170

$$D_L = \frac{\sum_{i=1}^{3} N_i D_i}{\sum_{i=1}^{3} N_i} = 6.1\,\text{cm} \quad \text{length average diameter} \tag{3.1}$$

$$D_A = \frac{\sum_{i=1}^{3} N_i D_i^2}{\sum_{i=1}^{3} N_i D_i} = 34.8 \text{ cm} \quad \text{area average diameter} \tag{3.2}$$

$$D_V = \frac{\sum_{i=1}^{3} N_i D_i^3}{\sum_{i=1}^{3} N_i D_i^2} = 60.9 \text{ cm} \quad \text{volume average diameter} \tag{3.3}$$

There then follows some appropriate averages. The length average diameter, D_L, is calculated to be 6.1 cm. The area average diameter, D_A, is 34.8 cm, and the volume average, D_V, is 60.9 cm. This last average suggests that the answer to the posed question might safely be no. A 60.9 cm steel ball has a mass of 930 kg. Note that the averages are related by particular summations. These same summation concepts are used to characterize polymer molecular weight averages.

3.2.2 Molecular Weight Distributions for Polymers

Commercial polymers are made up of molecules of differing molecular weight as discussed in Chapter 2. The shape of a typical commercial polymer molecule can be as a first approximation considered a "Gaussian spherical" shape in the undisturbed melt or solvent with a size proportional to the number of atoms in the molecule. Design engineers are interested in a number of properties: tensile strength, melt elasticity, and power to operate the production extruder; all are functions of different polymer average molecular weights. Thus it follows, when describing the molecular weight of a polymer, that the appropriate average must be used when dealing with the distribution of polymer molecular sizes in typical polymer melts, solutions, or solids in order to understand how the polymer responds to environmental forcing functions like shear, normal stress, strain or strain rate, and elongational strain.

The two most common average molecular weights of polymers are the number average, M_n, and the weight average, M_w, molecular weight. The number average molecular weight, M_n, is defined as the total weight divided by the total number molecules. The following summation is the mathematical representation of M_n:

$$M_n = \frac{\sum_{i=1}^{n} N_i M_i}{\sum_{i=1}^{n} N_i} \tag{3.4}$$

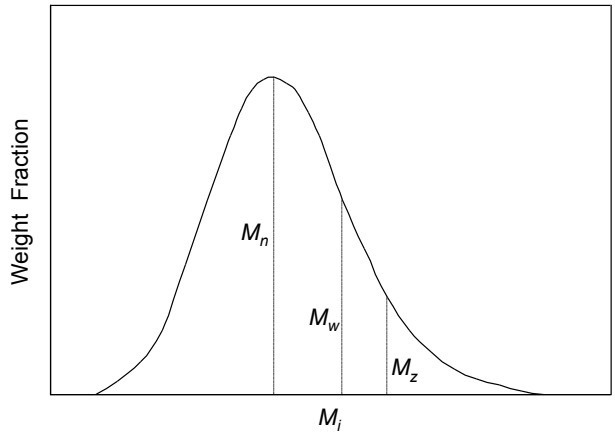

Figure 3.1 Schematic of a molecular weight distribution and the number average, weight average, and *z* average molecular weights

where N_i is the number of molecules with a molecular weight of M_i. As expected, the number average molecular weight is related to the number of molecules (the summation in the denominator), and it is therefore a colligative property of the material. It can thus be directly measured by techniques such as osmotic pressure, freezing point depression, and the boiling point increase of a good solvent. The number average molecular weight often correlates well with the tensile strength and impact properties of a polymer family. The number average molecular weight is also the first moment of the molecular weight distribution function. Discussion of moments of distributions can be found in texts on the introduction to statistics. The number average molecular weight is at the maximum of the differential representation of a molecular weight chromatogram, as shown in Figure 3.1. This figure is a representation that illustrates how the molecular weight averages are related to the molecular weight distribution; that is, the distribution of molecular sizes in a polymer sample. There are a few techniques for obtaining a distribution of the polymer molecular weights, including but not limited to gel permeation chromatography, high-pressure liquid chromatography, and temperature-rising elution fractionation for crystalline polymers. These techniques and others are presented for PE resins in reference [32]. The number average molecular weight is located at the maximum for the weight fraction, W_i, distribution, and the weight average and *z* average molecular weights are at higher molecular weights in distribution, as shown in Figure 3.1. The weight fraction is calculated using Equation 3.5, and the sum of the weight fractions must equal one by definition.

$$W_i = \frac{N_i M_i}{\sum_{j=1}^{n} N_j M_j} \tag{3.5}$$

$$1 = \sum_{i=1}^{n} W_i \tag{3.6}$$

The weight average molecular weight, M_w, is the second moment of the distribution and calculated from the distribution as follows:

$$M_w = \frac{\sum_{i=1}^{n} N_i M_i^2}{\sum_{i=1}^{n} N_i M_i} \tag{3.7}$$

The weight average molecular weight is always equal to or larger than the number average molecular weight. Since it is based on the size or the mass of the molecules, the weight average molecular weight can be directly measured with techniques that include light scattering and ultracentrifugation. The weight average molecular weight correlates with the Newtonian viscosity of many polymers. For example, the higher the weight average molecular weight of a polymer, the higher the Newtonian viscosity will be at limiting flow rates for the same number average molecular weight. This correlation will be discussed later in the chapter.

The third important average molecular weight is the third moment or the *z* average molecular weight, M_z. This average is calculated from the molecular weight distribution as follows:

$$M_z = \frac{\sum_{i=1}^{n} N_i M_i^3}{\sum_{i=1}^{n} N_i M_i^2} \tag{3.8}$$

The *z* average molecular weight has been found to correlate with the shear viscosity of polymer melts when the molecular weight distribution is very broad and where very large molecules appear to dominate the resistance to fluid flow.

Another important molecular weight concept is the polydispersity index (*PI*). This index is defined as the ratio of the weight average molecular weight divided by the number average molecular weight. It is a first-order attempt to characterize the broadness of the molecular weight distribution. This ratio is always greater than or equal to 1. Sometimes a polymer is labeled as monodispersed with a polydispersity index of exactly 1. These polymers, however, usually have a polydispersity index of 1.01 to 1.1. The polydispersity index is related to the effect of shear rate on the measured viscosity of polymer melts that have a molecular weight greater than the so-called critical molecular weight, M_c. As the polydispersity index increases the viscosity becomes shear-rate dependent at lower shear rates, or narrow distribution polymers have higher viscosity for a wider shear rate range.

Polymer molecular weight, branching, molecular weight distribution, and the rheological characteristics of polymers are therefore very interdependent.

$$PI = \frac{M_w}{M_n} \tag{3.9}$$

Finally, a solvent viscosity method is often used to measure the molecular weight of many polymers such as PET, and this viscosity average molecular weight is often close to the weight average molecular weight.

3.3 Basic Rheology Concepts

Materials are modeled classically as either viscous, such as water or molasses, or elastic in nature, such as steel beams or metal springs. In general, polymers are complex materials that behave in a combined response to strain with both viscous and elastic characteristics. Under conditions where the material exhibits both viscous and elastic rheological behavior, the polymers are described as viscoelastic. That is, polymers have substantial viscous and elastic characteristics when strained.

Although polymers exhibit both viscous and elastic responses at all temperatures, the elastic response is particularly strong at temperatures less than 50 °C above the glass transition temperature, particularly for polymers well above their critical molecular weight. Polymers are often considered to have dominant viscous rheological responses if they are stressed at temperatures over 100 °C above the glass transition temperature for amorphous polymers or 100 °C above the crystalline melting point for semicrystalline resins.

Elastic and viscous characteristics of materials can be visualized using a Cartesian material element, as shown in Figure 3.2. For this visualization the square shape in the *x-y* plane is deformed into a parallelogram. A force is applied to the material element parallel to one axis, in this case along the *x* axis at a distance *H* up the *y* axis. The material element is deformed away from the *y* axis by a distance *a* by the force *F*.

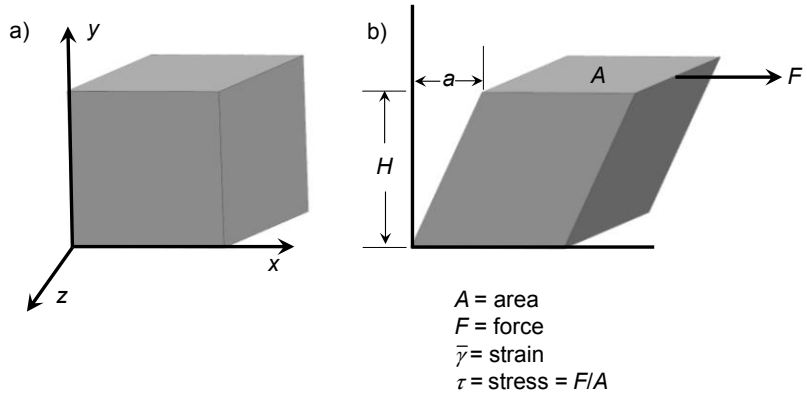

Figure 3.2 Response to elastic deformation of a solid: a) material element without an applied force, and b) solid deformation and the elastic response to an applied force

For this solid the velocity is zero. This is thus a static situation. The strain can be calculated along with the stress:

$$\bar{\gamma} = \frac{a}{H} \tag{3.10}$$

$$\tau = \frac{F}{A} \tag{3.11}$$

where A is the surface area for the exerted force F, $\bar{\gamma}$ is the strain, and τ is the stress. It is important to note that this analysis is only valid for infinitesimally small local deformations.

The evaluation of viscosity is similar to the evaluation of elastic deformation except the stress in the element changes due to the local velocity gradient. The time variable is defined as the strain rate. The element changes its shape as a function of time, while the strain-rate-induced stress is present. Viscosity is the local slope of the function relating stress in the element to strain rate. The usual functionality is found in Figure 3.3. The process can be visualized by a constant force on the top of the element that creates a strain rate throughout the element. This strain rate causes each molecular layer of the material to move relative to the adjacent layer continuously. Obviously the element is suspended in a continuum and material flows into and out of the geometric element.

For this simple geometry the shear rate, $\dot{\gamma}$, is equal to the difference between the velocity at the top of the element, U, and the velocity at the bottom of the element, zero, divided by the height of element H. The shear stress is again $\tau = F/A$, the element surface area divided by the force. The viscosity, η, is the ratio of shear stress, τ, divided by shear rate, $\dot{\gamma}$, at any shear rate, $\eta = \tau/\dot{\gamma}$. For Newtonian materials such as water, molasses, or gasoline at the nominal shear rates found in everyday